Modeling Rotorcraft Dynamics with Finite Element Multibody Procedures*

Olivier A. Bauchau
Georgia Institute of Technology, School of Aerospace Engineering
Atlanta, GA, USA

Carlo L. Bottasso
Dipartimento di Ingegneria Aerospaziale, Politecnico di Milano
Milano, Italy

Yuri G. Nikishkov
Georgia Institute of Technology, School of Aerospace Engineering
Atlanta, GA, USA

Abstract

This paper describes a multibody dynamics approach to the modeling of rotorcraft systems and reviews the key aspects of the simulation procedure. The multibody dynamics analysis is cast within the framework of nonlinear finite element methods, and the element library includes rigid and deformable bodies as well as joint elements. No modal reduction is performed for the modeling of flexible bodies. The structural and joint element library is briefly described. The algorithms used to integrate the resulting equations of motion with maximum efficiency and robustness are discussed. Various solution procedures, static, dynamic, stability, and trim analysis, are presented. Post-processing and visualization issues are also addressed. Finally, the paper concludes with selected rotorcraft applications.

1 Introduction

Multibody dynamics analysis was originally developed as a tool for modeling mechanisms with simple tree-like topologies composed of rigid bodies, but has considerably evolved to the point where it can handle nonlinear flexible systems with arbitrary topologies. It is now widely used as a fundamental design tool in many areas of mechanical engineering. In the automotive industry, for instance, multibody dynamics analysis is routinely used for optimizing vehicle ride qualities, a complex multidisciplinary task that involves the simulation of many different sub-components. Modern multibody codes can deal with complex mechanisms of arbitrary topologies including sensors, actuators and controls, are interfaced with CAD solid modeling programs that allow to directly import the problem geometry, and have sophisticated graphics, animation and post-processing features [1, 2]. The success of multibody dynamics analysis tools stems from their flexibility: a given mechanism can be modeled by an idealization process that identifies the mechanism components from within a large library of elements implemented in the code. Each element provides a basic

Mathematical and Computer Modeling, **33**, pp 1113-1137, 2001.

functional building block, for example a rigid or flexible member, a hinge, a motor, etc. Assembling the various elements, it is then possible to construct a mathematical description of the mechanism with the required level of accuracy.

Despite its generality and flexibility, multibody dynamics analysis has not yet gained acceptance in the rotorcraft industry. Historically, the classical approach to rotor dynamics has been to use a modal reduction approach, as pioneered by Houbolt and Brooks [3]. Typical models were limited to a single articulated blade connected to an inertial point, and the control chain was ignored. The equations of motion were specifically written for a blade in a rotating system, and ordering schemes were used to decrease the number of nonlinear terms [4]. In time, more detailed models of the rotor were developed to improve accuracy and account for various design complexities such as gimbal mounts, swash-plates, or bearingless root retention beams, among many others. The relevant equations of motion were derived for the specific configurations at hand. In fact, the various codes developed in-house by rotorcraft manufacturers are geared towards the modeling of the specific configuration they produce. This approach severely limits the generality and flexibility of the resulting codes. In recent years, a number of new rotorcraft configurations have been proposed: bearingless rotors with redundant load paths, tilt rotors, variable diameter tilt rotors, and quad rotors, to name just a few. Developing a new simulation tool for each novel configuration is a daunting task, and software validation is an even more difficult issue. Furthermore, the requirement for ever more accurate predictions calls for increasingly detailed and comprehensive models. For instance, modeling the interaction of the rotor with a flexible fuselage or with the control chain must be considered in order to capture specific phenomena or instabilities.

Clearly, a more general and flexible paradigm for modeling rotorcraft systems is needed. It seems that many of the concepts of multibody dynamics analysis would be readily applicable to the rotorcraft dynamics analysis, since a rotorcraft system can be viewed as a complex flexible mechanism. In particular, the ability to model novel configurations of arbitrary topology through the assembly of basic components chosen from an extensive library of elements is highly desirable. In fact, this approach is at the heart of the finite element method which has enjoyed, for this very reason, an explosive growth in the last few decades. This analysis concept leads to new comprehensive simulation software tools that are modular and expandable. Modularity implies that all the basic building blocks can be validated independently, easing the more challenging task of validating complete simulation procedures. Because they are applicable to configurations with arbitrary topologies, including those not yet foreseen, such simulation tools will enjoy a longer life span, a critical requirement for any complex software tool.

Fig. 1 depicts the conceptual representation of a rotorcraft system as a flexible multibody system. The various mechanical components of the system are associated with the elements found in the library of typical multibody analysis tools. The picture shows a classical configuration for the control chain, consisting of a swash-plate with rotating and non-rotating components. The lower swash-plate motion is controlled by actuators that provide the vertical and angular control inputs. The upper swash-plate is connected to the rotor shaft through a scissors-like mechanism, and controls the blade pitching motions through pitch-links. This familiar control linkage configuration can be modeled using the following elements: rigid bodies, used to model the lower and upper swash-plate components and scissors links, and beams for modeling the flexible shaft and pitch-link. These bodies are connected through standard mechanical joints: a hinge, called a *revolute joint* in the terminology of multibody dynamics [1, 2], connects the upper and lower swash-plates, allowing the former to rotate at the shaft angular velocity while the latter is non-rotating. Revolute joints also connect the scissors links to each other and to the upper swash-plate, thereby synchronizing the shaft and upper swash-plate. Other types of joints are required for the model. For instance, the lower swash-plate is allowed to tilt with respect to an element that slides along the shaft, but does not rotate about the shaft direction. The *universal joint*, a sequence of two revolute joints whose mutually orthogonal axes of rotation lie in a common plane, serves this purpose. Similarly, the

pitch-link is connected to the pitch-horn by means of a *spherical joint* that allows the connected components to be at an arbitrary orientation with respect to each other.

Fig. 1 also shows two different rotor configurations: a classical, fully articulated design on the right and a bearingless design on the left. The articulated blade is connected to the hub through three revolute joints, that model the flap, lag and pitch hinges. Possible offsets between these joints could be modeled by means of rigid or flexible bodies. The blade itself is modeled by an appropriate beam element that should account for the inertial and elastic couplings that arise from the use of composite materials [5]. The bearingless design is a multiple load path configuration, involving a flex-beam and a torsion cuff assembled in parallel and connected by a snubber. It is important to note that the two designs, fully articulated or bearingless, can be modeled by assembling different sets of elements from the multibody library of elements. There is no need to derive and validate two different sets of equations for the two configurations. Of course, the level of detail presented in fig. 1 is not always needed: some or all of the control chain components could be omitted, and the blade could be represented by rigid bodies rather than beam elements, if a crude model is desired.

This paper describes a multibody dynamics approach to the modeling of rotorcraft system and reviews the key aspects of the simulation procedure. The proposed approach provides the level of generality and flexibility required to solve complex problems such as those described in the above conceptual examples. The multibody dynamics analysis is cast within the framework of nonlinear finite element methods, and the element library includes rigid and deformable bodies as well as joint elements. Deformable bodies are modeled with the finite element method, in contrast with the classical approach to multibody dynamics, that predominantly relies on rigid bodies or introduces flexibility by means of a modal representation [6, 7]. With today's advances in computer hardware, very inexpensive PCs provide enough computational power to run full finite element models of complex rotor systems. Hence, resorting to modal reduction in order to save CPU time is no longer a valid argument, specially when considering the possible loss of accuracy associated with this reduction [8].

In the proposed approach, the formulations of beams and shells are geometrically exact, *i.e.* they account for arbitrarily large displacements and finite rotations, but are limited to small strains. The equations of equilibrium are written in a Cartesian inertial frame. Constraints are modeled using the Lagrange multiplier technique. This leads to systems of equations that are highly sparse, although not of minimal size. This approach can treat arbitrarily complex topologies. Furthermore, because it is an extension of the finite element method to multibody systems, the algorithms such as sparse solvers, and data structures developed for FEM analysis are directly applicable to the present approach.

The paper is organized as follows. Section 2 presents the element library comprising structural and joint elements. Section 3 reviews the algorithms that have been developed to integrate the equations of motion with maximum efficiency and robustness. Section 4 deals with the solution procedures: static, dynamic, stability, and trim analysis can be performed. Post-processing and visualization issues are addressed in section 5. The paper concludes with selected rotorcraft applications presented in section 6.

2 Element Library

The element library involves structural elements: rigid bodies, composite capable beams and shells, and joint models. Although a large number of joint configurations are possible, most applications can be treated using the well known lower pair joints presented here. More advanced joints, such as sliding joints and backlash elements are briefly described. Examples of how these various elements are used to model practical rotorcraft configurations will be given; additional examples are described in section 6. Finally, possible approaches for coupling multibody systems with aerodynamic models

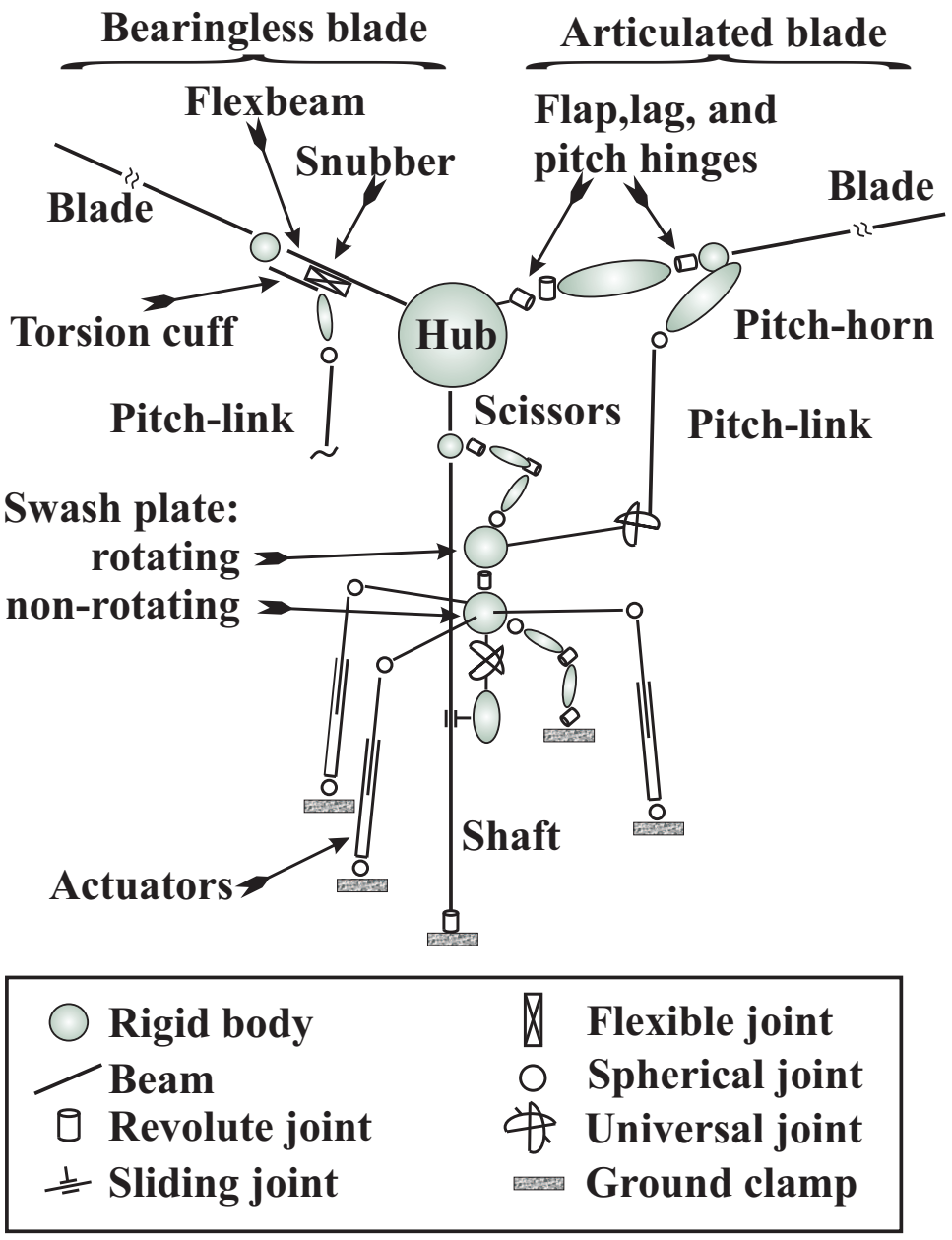

Figure 1: Detailed multibody representation of a rotor system. At right, a typical articulated blade. At left, a bearingless blade design.

are presented.

2.1 Beam, Shell and Rigid Body Models

Rigid body and beam models are the heart of rotorcraft multibody models. Shell models are also useful for dealing with composite flex-beams in bearingless rotors [9, 10]. Rigid bodies, beams and shells are all characterized by the presence of linear and rotational fields. In the proposed formulation, all elements are referred to a single inertial frame, and hence, arbitrarily large displacements and finite rotations must be treated exactly.

Rigid bodies can be used for modeling components whose flexibility can be neglected or for introducing localized masses. For example, in certain applications, the flexibility of the swashplate may be negligible and hence, a rigid body representation of this component is acceptable; the model consists of two rigid bodies, representing the rotating and the non-rotating components, respectively, properly connected to each other and to the rest of the control chain.

Beams are typically used for modeling rotor blades, but can also be useful for representing transmissions shafts, pitch links, or wings of a tilt rotor aircraft. In view of the increasing use of composite materials in rotorcraft, the ability to model components made of laminated composite materials is of great importance. Specifically, it must be possible to represent shearing deformation effects, the offset of the center of mass and of the shear center from the beam reference line, and all the elastic couplings that can arise from the use of tailored composite materials. Most multibody codes are unable to deal with such structures with a sufficient level of accuracy.

In the work of Berdichevsky [11], the three-dimensional elasticity representation of a beam was shown to give rise to two separate problems. The first problem is a linear, two-dimensional problem over the beam cross-section which provides a set of elastic constants characterizing the beam cross-section and a set of "recovery relations" relating the three-dimensional displacements, strain, and stress fields in the beam to generalized one-dimensional strain measures. The second problem is a nonlinear, one-dimensional problem along the beam reference line that predicts the nonlinear response of the beam when subjected to time dependent loads. These two analysis work together to provide a methodology for the simulation of multibody systems involving beams made of anisotropic materials. At first, the sectional properties of the beam are computed based on a linear, two-dimensional finite element analysis of the beam cross-section. These properties are used to define the physical characteristics of the beams involved in the multibody system. Next, the dynamic response of the multibody system is computed using a nonlinear, finite element procedure. At the post-processing stage, the predicted generalized strain measures are used in conjunction with the recovery relations to evaluate the beam three-dimensional displacement, stress, and strain distributions.

An extension of this methodology to generally anisotropic and inhomogeneous beams was undertaken by Cesnik and Hodges [12]. Results from application of this approach are very similar to those obtained from application of the pioneering work of [13]. The splitting of the three-dimensional problem into two- and one-dimensional parts results in a tremendous savings of computational effort relative to the cost of three-dimensional finite element analysis, the only alternative for realistic beams. The one-dimensional equations that fall out from this approach are the canonical intrinsic equations of motion for beams, as developed by many investigators [14, 15, 16, 17, 18]. Ref. [5] gives details and examples of application of the integration of the cross-sectional analysis procedure with the multibody dynamic simulation.

A similar approach can be developed for composite shell models with couplings [19]. In this case, a one-dimensional through-the-thickness analysis provides the elastic constants, that are then used as input for the classical nonlinear two-dimensional analysis of dynamic equilibrium defined for the shell reference surface. A unified view on geometrically exact beams and shells is found in [20].

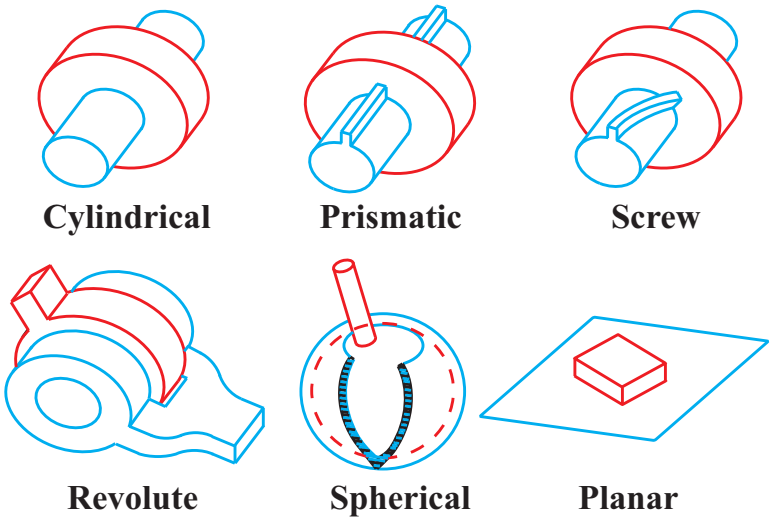

Figure 2: The six lower pairs.

2.2 Joint Models

A distinguishing feature of multibody systems is the presence of a number of joints that impose constraints on the relative motion of the various bodies of the system. Most joints used for practical applications can be modeled in terms of the so called *lower pairs* [21]: the revolute, prismatic, screw, cylindrical, planar and spherical joints, depicted in fig. 2. Articulated rotors and their kinematic chains are easily modeled with the help of lower pair joints. For example, a conventional blade articulation can be modeled with the help of three revolute joints representing pitch, lag and flap hinges. Another example is provided by the pitch-link, which is connected to the pitch-horn by means of a spherical joint, and to the upper swash-plate by a universal joint to eliminate rotation about its own axis.

The kinematics of lower pair joints can be described in terms of two Cartesian frames $X^A = [\underline{E}_1^A, \underline{E}_2^A, \underline{E}_3^A]$ and $X^B = [\underline{E}_1^B, \underline{E}_2^B, \underline{E}_3^B]$, and two position vectors $\underline{R}^A = \underline{R} + \underline{u}^A$ and $\underline{R}^B = \underline{R} + \underline{u}^B$. $\underline{R}^A$ and X^A represent the position and orientation of a point on a rigid or flexible body denoted body A, whereas $\underline{R}^B$ and X^B are the corresponding quantities for body B. If the two bodies are rigidly connected to one another, their six relative motions, three displacements and three rotations, must vanish at the connection point. If one of the lower pair joints connects the two bodies, one or more relative motions will be allowed.

Let d_i be the relative displacement between the two bodies in the direction aligned with $\underline{E}_i^A$, and θ_i the relative rotation about $\underline{E}_i^A$. Table 1 then formally defines the six lower pairs in terms of the relative displacement and/or rotation components that can be either free or constrained to a null value. The six lower pairs are graphically depicted in fig. 2.

All lower pair constraints can be expressed by one of the following two equations

$$\underline{E}_i^A \cdot (\underline{u}^A - \underline{u}^B) - d_i = 0, \tag{1}$$

$$\cos\theta_i \, (\underline{E}_j^A \cdot \underline{E}_k^B) - \sin\theta_i \, (\underline{E}_k^A \cdot \underline{E}_k^B) = 0. \tag{2}$$

The first equation constrains the relative displacement if $d_i = 0$, whereas if d_i is a free variable it defines the unknown relative displacement in that direction. Similarly, the second equation either constrains the relative rotation if $\theta_i = 0$, or defines the unknown relative rotation θ_i if it is a free variable.

The explicit definition of the relative displacements and rotations in a joint as additional unknown variables represents an important detail of the implementation. First of all, it allows the

	Relative displacements			Relative rotations		
Joint type	d_1	d_2	d_3	θ_1	θ_2	θ_3
Revolute	No	No	No	No	No	Yes
Prismatic	No	No	Yes	No	No	No
Screw	No	No	$= p\theta_3$	No	No	Yes
Cylindrical	No	No	Yes	No	No	Yes
Planar	Yes	Yes	No	No	No	Yes
Spherical	No	No	No	Yes	Yes	Yes

Table 1: Definition of the six lower pair joints. "Yes" or "No" indicate that the corresponding relative motion is allowed or inhibited, respectively. For the screw joint, p is the screw pitch.

introduction of generic spring and/or damper elements in the joints, as usually required for the modeling of realistic configurations. Second, the time histories of joint relative motions can be driven according to suitably specified time functions. For example, in a helicopter rotor, collective and cyclic pitch settings can be obtained by prescribing the time history of the relative rotation at the corresponding joints.

In the classical formulation of prismatic joints for rigid bodies, kinematic constraints are enforced between the kinematic variables of the two bodies, see eqs. (1) and (2). These constraints express the conditions for relative translation of the two bodies along a body fixed axis, and imply the relative sliding of the two bodies which remain in constant contact with each other. However, these kinematic constraints no longer imply relative sliding with contact when one of the bodies is flexible. To remedy this situation, a *sliding joint* [22, 23] was proposed that involves kinematic constraints at the instantaneous point of contact between the sliding bodies. This more sophisticated type of constraint is required for the accurate modeling of specific rotorcraft components. Consider, for instance, the sliding of the swash-plate on the rotor shaft, or the sliding joints involved in the retraction mechanism of the variable diameter tilt rotor [24].

Backlash behavior can be added to the modeling of revolute joints characterized by eq. (2). The joint is generally free to rotate, but when the relative rotation reaches a preset value, a unilateral contact condition is activated corresponding to the backlash "stop." The associated contact force is computed according to a suitable contact force model. Unilateral contact conditions and contact force models are routinely used in multibody dynamics for the modeling of contact/impact phenomena [25, 26, 27]. This element can be used to model the blade droop stops.

2.3 Aerodynamic Models

A description of the various aerodynamic solution procedures used for the modeling of rotorcraft is beyond the scope of this paper. Simplified models based on lifting line theory and vortex wake models, or sophisticated computational fluid dynamics codes can be used for this purpose. At each time step of the simulation, the aerodynamic loads acting on the blades and wings must be computed based on the present configuration of the system, and are then used to evaluate the dynamic response. More details concerning the coupling strategies can be found in refs. [28, 29].

3 Robust Integration of Multibody Dynamics Equations

From the description given so far, it is clear that the equations governing nonlinear flexible multibody systems present very specific features. First, they are highly nonlinear. There are several possible sources of nonlinearities: large displacements and finite rotations (geometric nonlinearities), or

nonlinear constitutive laws for the deformable components of the system (material nonlinearities). Second, when constraints are modeled via the Lagrange multiplier technique, the resulting equations present a dual differential/algebraic (DAE) nature. Third, the exact solution of the equations of motion implies the preservation of a number of dynamic invariants, such as energy and momenta. Fourth, when the elastic bodies of the system are modeled by means of an appropriate spatial discretization process, such as the finite element method, high frequency modes are introduced in the system. Note that these high frequency modes are artifacts of the discretization process, and bear no physical meaning. In large systems, numerical round-off errors are sufficient to provide significant excitation of these modes, hindering the convergence process for the solution of the nonlinear equations of motion. Furthermore, the nonlinearities of the system provide a mechanism to transfer energy from the low to the high frequency modes. Hence, the presence of high frequency numerical dissipation is an indispensable feature of robust time integrators for multibody systems.

All these features of multibody systems must be carefully considered and specifically taken into consideration when developing robust simulation procedures that are applicable to a wide spectrum of applications. In particular, problems related to the modeling of helicopters put stringent requirements on the accuracy and robustness of integration schemes. Indeed, rotors are characterized by highly nonlinear dynamics, large numbers of constraints, especially when the entire control chain is modeled, highly flexible members, large number of degrees of freedom, and widely different spatial and temporal scales. On this last issue, consider, for instance, the dramatic difference between the axial and flap-wise bending stiffnesses of a typical rotor blade.

The classical approach to the numerical simulation of flexible multibody systems is generally based on the use of off-the-shelf, general purpose DAE solver. DAE integrators are specifically designed for effectively dealing with the dual differential/algebraic nature of the equations, but are otherwise unaware of the specific features and characteristics of the equations being solved. Although appealing because of its generality, this approach implies that the special features that were just pointed out will be approximated in various manners. For example, index reduction methods [30] transform the holonomic constraints into velocity or acceleration constraints, thus introducing the drift phenomenon, *i.e.* the numerical solution is allowed to drift away from the level set defined by the holonomic constraints. Similarly, the preservation of the dynamic invariants, such as the system energy, is usually ignored.

While this standard procedure performs adequately for a number of simulations, alternate procedures have been developed [18, 20]. Instead of applying a suitable integrator to the equations modeling the dynamics of multibody systems, algorithms are *designed* to satisfy a number of precise *requirements*. These design requirements are carefully chosen in order to convey to the numerical method the most important features of the equations being solved. In particular, the following requirements will be satisfied by the proposed approach: *nonlinear unconditional stability* of the scheme, a *rigorous treatment of all nonlinearities*, the *exact satisfaction of the constraints*, and the presence of *high frequency numerical dissipation*. The proof of nonlinear unconditional stability stems from two physical characteristics of multibody systems that will be reflected in the numerical scheme: the preservation of the total mechanical energy, and the vanishing of the work performed by constraint forces. Numerical dissipation is obtained by letting the solution drift from the constant energy manifold in a controlled manner in such a way that at each time step, energy can be dissipated but not created.

Algorithms meeting the above design requirements can be obtained through the following process. First, a discretization scheme for flexible members of the system is developed that preserves the total mechanical energy of the system at the discrete solution level. Then, a discretization process is obtained for the constraint reactions associated with the holonomic and non-holonomic constraints imposed on the system. Constraint reactions are discretized in a manner that guarantees the satisfaction of the nonlinear constraint manifold, *i.e.* the constraint condition will not drift. At the same time, the discretization implies the vanishing of the work performed by the forces of

constraint at the discrete solution level. Consequently, the discrete energy conservation laws proved for the flexible members of the system are not upset by the introduction of the constraints. The resulting Energy Preserving (EP) scheme provides nonlinear unconditional stability for nonlinear, flexible multibody systems. However, this scheme lacks the indispensable high frequency numerical dissipation required to tackle realistic engineering problems.

In a second phase, a new discretization, closely related to the EP scheme, is developed for the flexible components of the system. This new discretization implies a discrete energy decay statement that results in high frequency numerical dissipation. The discretization of the forces of constraint is also closely related to that of the EP scheme and presents identical properties: no drift of the constraint conditions and vanishing of the work they perform. Here again, the introduction of constraints does not upset the discrete energy decay law. The resulting Energy Decaying (ED) scheme satisfies all the design requirements set forth earlier, and is therefore ideally suited for the simulation of nonlinear, flexible multibody systems. More details on ED schemes can be found in refs. [16, 31, 32, 17, 33, 34, 35, 18, 20]. In particular, ref. [20] presents a variant of the ED scheme that allows for user-tunable numerical dissipation, through a single scalar parameter that is directly related to the scheme spectral radius.

4 Solution Procedures

Once a multibody representation of a rotorcraft system has been defined, several types of analysis can be performed on the model. The main features of the static, dynamic, stability, and trim analysis are briefly discussed in the following sections.

4.1 Static Analysis

The static analysis solves the static equations of the problem, *i.e.* the equations resulting from setting all time derivatives equal to zero. The deformed configuration of the system under the applied static loads is then computed. The static loads are of the following type: prescribed static loads, steady aerodynamic loads, and the inertial loads associated with prescribed rigid body motions. In that sense, hover can be viewed as a static analysis.

Once the static solution has been found, the dynamic behavior of small amplitude perturbations about this equilibrium configuration can be studied: this is done by first linearizing the dynamic equations of motion, then extracting the eigenvalues and eigenvectors of the resulting linear system. Due to the presence of gyroscopic effects, the eigenpairs are, in general, complex. For typical rotor blade, the real part of the eigenvalues is negligible, whereas for transmission shafts, this real part is large and provides information about the stability of the system. Finally, static analysis is also useful for providing the initial conditions to a subsequent dynamic analysis.

4.2 Dynamic Analysis

The dynamic analysis solves the nonlinear equations of motion for the complete multibody system. The initial condition are taken to be at rest, or those corresponding to a previously determined static or dynamic equilibrium configuration.

Complex multibody systems often involve rapidly varying responses. In such event, the use of a constant time step is computationally inefficient, and crucial phenomena could be overlooked due to insufficient time resolution. Automated time step size adaptivity is therefore an important part of the dynamic analysis solution procedure. In the context of the energy decaying schemes discussed in Section 3, a simple but effective way of deriving the time adaptivity process was proposed in ref. [34]. The numerically dissipated energy, a positive-definite function of the velocity and strain fields of the

entire system, will clearly be null for the exact solution of the problem, and its magnitude can be used as a measure of the error associated with the time discretization process. For a single degree of freedom linear oscillator, the relationship between the amount of dissipated energy and the time step size can be obtained analytically. This explicit relation was found to yield an estimate of the time step size required to achieve a desired level of error with adequate accuracy. All the results presented in Section 6 make use of this simple error estimator.

4.3 Stability Analysis

An important aspect of aeroelastic response of rotorcraft is the potential presence of instabilities which can occur both on the ground and in the air. Typically, Floquet theory is used for this purpose because the system presents periodic coefficients. Floquet theory requires the computation of the Floquet transition matrix which relates all the states of the system at a given instant to the same states one period later. The size of this transition matrix is equal to the total number of states of the system. Stability of the system is then related to the eigenvalues of this transition matrix.

Application of Floquet theory to rotorcraft problem has been limited to systems with a relatively small number of degrees of freedom. Indeed, as the number of degrees of freedom increases, the computational burden associated with the evaluation of the transition matrix becomes overwhelming. Typically, the columns of the transition matrix are computed one at a time, and correspond to the responses of the system after one period to linearly independent initial conditions. As a result, the computation of the transition matrix of a system with N states requires N integrations of the system response over one period, for a set of N linearly independent initial conditions. Nevertheless, this approach has been widely used for the assessment of stability of small dimensional systems with periodic coefficients [36].

The computational cost associated with the evaluation of the transition matrix becomes overwhelming when $N > 100$. As a result, stability analysis is typically performed on simplified models with the smallest number of degrees of freedom required to capture the physical phenomenon that causes the instability. When the system is stable, the evaluation of damping levels in the least damped modes becomes critical. These damping levels depend on all the forces acting on the rotor, and an accurate estimate of these loads is critical to obtain an accurate estimate of damping levels.

A novel approach has been proposed, the *implicit Floquet analysis* [37, 38], which evaluates the dominant eigenvalues of the transition matrix using the Arnoldi algorithm, without the explicit computation of this matrix. This method is far more computationally efficient than the classical approach and is ideally suited for systems involving a large number of degrees of freedom. The implicit Floquet analysis can be viewed as a post-processing step: all that is required is to predict the response of the system to a number of given initial conditions. Hence, it can be implemented using the proposed multibody dynamics formulation.

4.4 Trim Analysis

The problem of rotorcraft trim involves both the search for a periodic solution to the nonlinear rotor equations and the determination of the correct control settings that satisfy some desired flight conditions. The determination of control settings is an important aspect of rotorcraft analysis as these settings are known to deeply affect the entire solution as well as stability boundaries [39].

The auto-pilot and discrete auto-pilot methods [40] are well suited for the solution of the trim configuration when the problem has been formulated using the proposed finite element based multibody dynamics analysis. The auto-pilot method modifies the controls so that the system converges to a trimmed configuration. Additional differential equations are introduced for computing the required control settings. The discrete auto-pilot approach modifies the control settings at each revolution only.

5 Post-Processing and Visualization

The finite element based, multibody dynamic analysis of rotorcraft proposed here generates massive amounts of data. Typical models involve thousands of degrees of freedom, and realistic simulations require thousands of time steps. Interpreting this large quantity of information is a daunting task, and the power of simulation tools can be harnessed only if efficient visualization tools are used to post-process the predicted response. In fact, visualization is an invaluable tool for better understanding of system behavior.

Objects of the multibody system can be viewed in symbolic manner to help model validation, or with associated predefined geometrical shapes to improve the realism to the visualization. For static analysis, step-by-step visualization is provided together with eigenmode animation. For dynamic analysis, the time dependent system configuration is displayed, and different vector-type attributes, such as linear or angular velocities, internal forces or moments, curvatures or strains, and aerodynamic forces or moments can be added. Finally, the animation of the Floquet transition matrix eigenmodes provide insight into instability mechanism when performing stability analysis.

6 Applications

The following applications are presented in this section: the stability analysis of an articulated rotor with a mast mounted sight, the conversion from hover to forward flight mode for a variable diameter tilt-rotor and the analysis of a supercritical tail rotor transmission.

6.1 Stability Analysis of an Articulated Rotor with Control Linkages and a Mast Mounted Sight

The first example deals with the stability analysis of a complex rotor system involving control linkages and a flexible shaft. Fig. 3 depicts, in a schematic manner, the topology of the overall system comprising the blades, control linkages, mast mounted sight, elastic shaft, scissors and swash-plate.

The swash-plate is represented by two rigid bodies, rotating and non-rotating, connected by a revolute joint. The non-rotating lower swash-plate is connected to the ground by means of a universal joint followed by a prismatic joint. The collective input signal is provided by prescribing the relative displacement of the prismatic joint, whereas the cyclic input signals are provided by prescribing the two relative rotations of the universal joint. The rotating upper swash-plate is connected to the pitch-links by means of universal joints. In turns, the pitch-links are attached to the pitch-horn through spherical joints and transfer the input control signals from the upper swash-plate to the blades. The rotation of the upper swash-plate is enforced by scissors that connect the upper swash-plate to the rotating shaft. The two part scissors are connected together, to the shaft, and to the upper swash-plate by means of revolute joints. The flexible shaft is attached to the hub, modeled as massive rigid body, that in turns, connects to the blades by root retention flexible beams. The mast-mounted sight also attaches to the rotor hub through a flexible post and revolute joint. A non-rotating stand pipe (not shown in fig. 3) connects the post to the ground, preventing rotation of the mast-mounted sight. The blades are connected to the root retention elements by three revolute joints with mutually orthogonal rotation axes that provide flap, lag, and pitch articulations.

Each blade was modeled with six cubic beam elements. The model included 36 beam elements, 32 joint elements and 31 rigid body elements, resulting in 910 degrees of freedom. The aerodynamic model was based on the dynamic inflow model developed by Peters [41]. Stability analysis involved 1347 states. Clearly, this system is of prohibitive size for classical Floquet analysis. The following

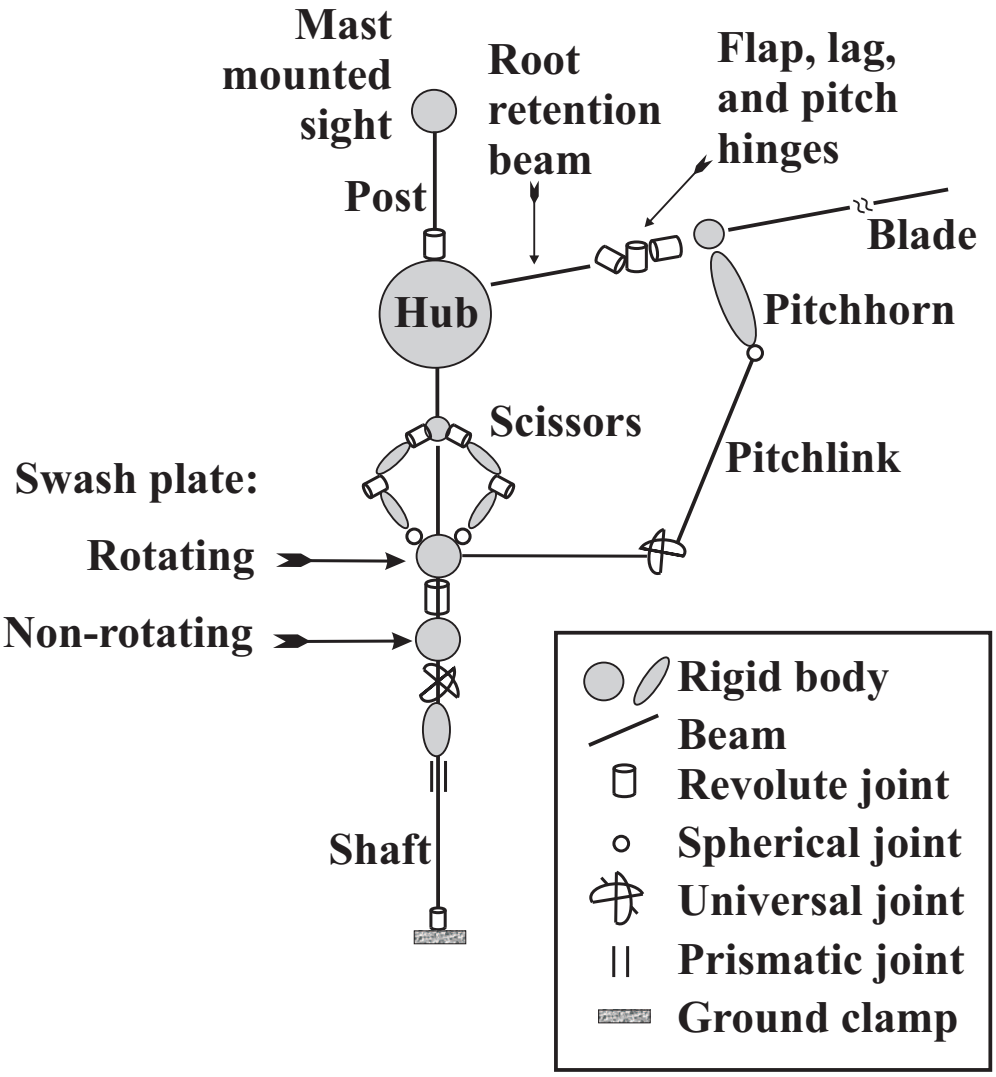

Figure 3: Configuration of articulated rotor with control linkages and a mast mounted sight. A single blade only is shown for clarity of the figure.

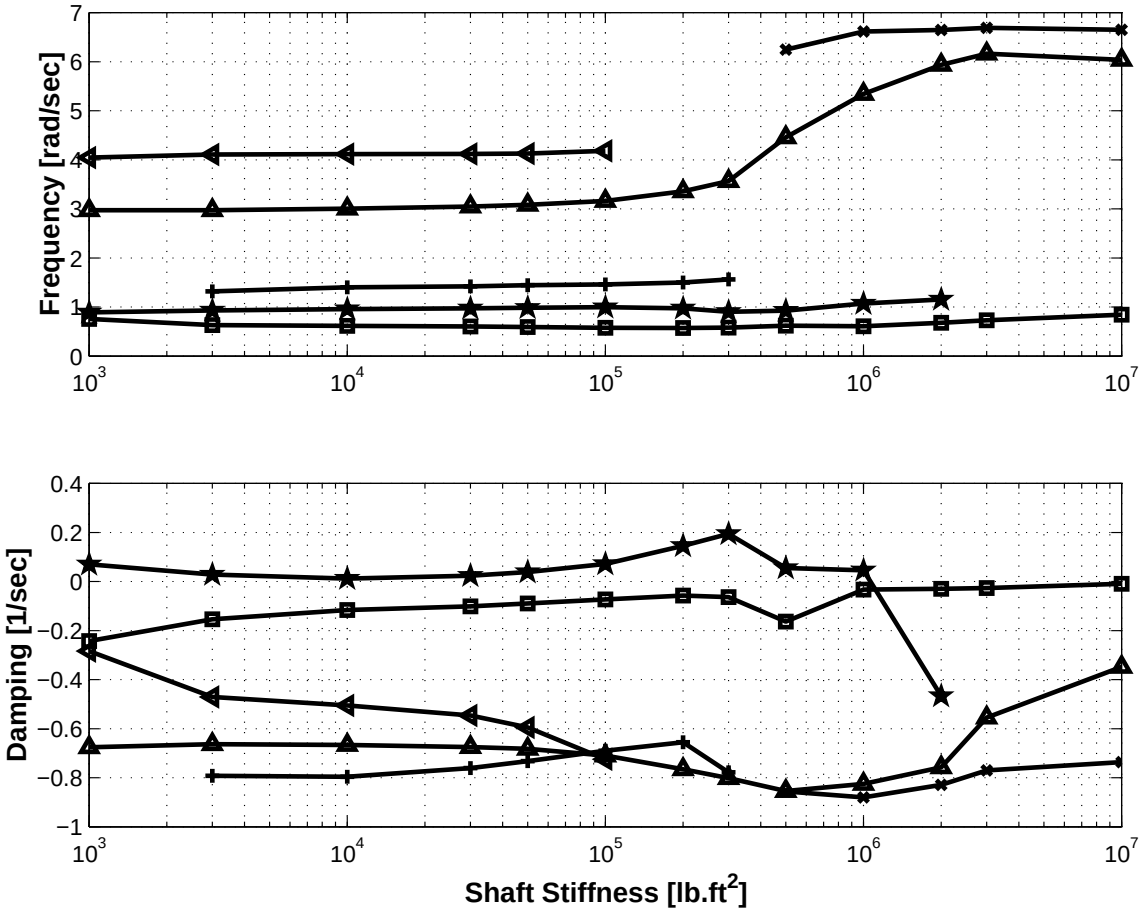

Figure 4: Frequencies and damping rates of the least-damped modes versus shaft bending stiffness.

control signals were used: collective amplitude $A^p = 0.0393$ ft (upward motion of the lower swash-plate prescribed as relative motion of the prismatic joint), cyclic amplitudes $A_1^u = 0.0172$ rad and $A_2^u = 0.0182$ rad (tilting motion of the lower swash-plate prescribed as relative rotations of the universal joint).

As the stiffness of the shaft decreases, the possibility of an instability arises. Indeed, the shaft tilting creates additional blade pitching due to the kinematics of the various interconnected linkages. These additional angles of attack then result in additional aerodynamic forces that can destabilize the system [42]. The implicit Floquet approach was used to evaluate the stability characteristics of this complex system. Fig. 4 shows the frequencies and damping rates of the least-damped modes versus shaft bending stiffness. The system is stable for high shaft stiffnesses. The instability appears for shaft stiffnesses below $I_s = 1 \times 10^6$ lb·ft^2 and for all stiffnesses below that critical value. Visualization of the eigenvector of the Floquet transition matrix provides insight into the mechanism of the instability. Fig. 5 shows the eigenvector of the transition matrix corresponding to the unstable eigenvalue at $I_s = 1 \times 10^6$ lb·ft^2. This mode involves a very significant bending motion of the elastic post; although less visible on the figure, motion of the pitch-links is also involved and generates blade twisting, that in turns, couples with the aerodynamic loading to cause the instability.

This type of instability is very hard to detect through a simple time simulation of the dynamic response of the system. Indeed, integration must be performed for a very large number of rotor revolutions before the instability manifests itself in the response output. Fig. 6 shows blade tip lag rotation in a rotating coordinate system and lag joint rotation for a 500 revolution simulation of the rotor system, at a shaft stiffness $I_s = 1 \times 10^6$ lb·ft^2. Even after 500 revolutions, the response of

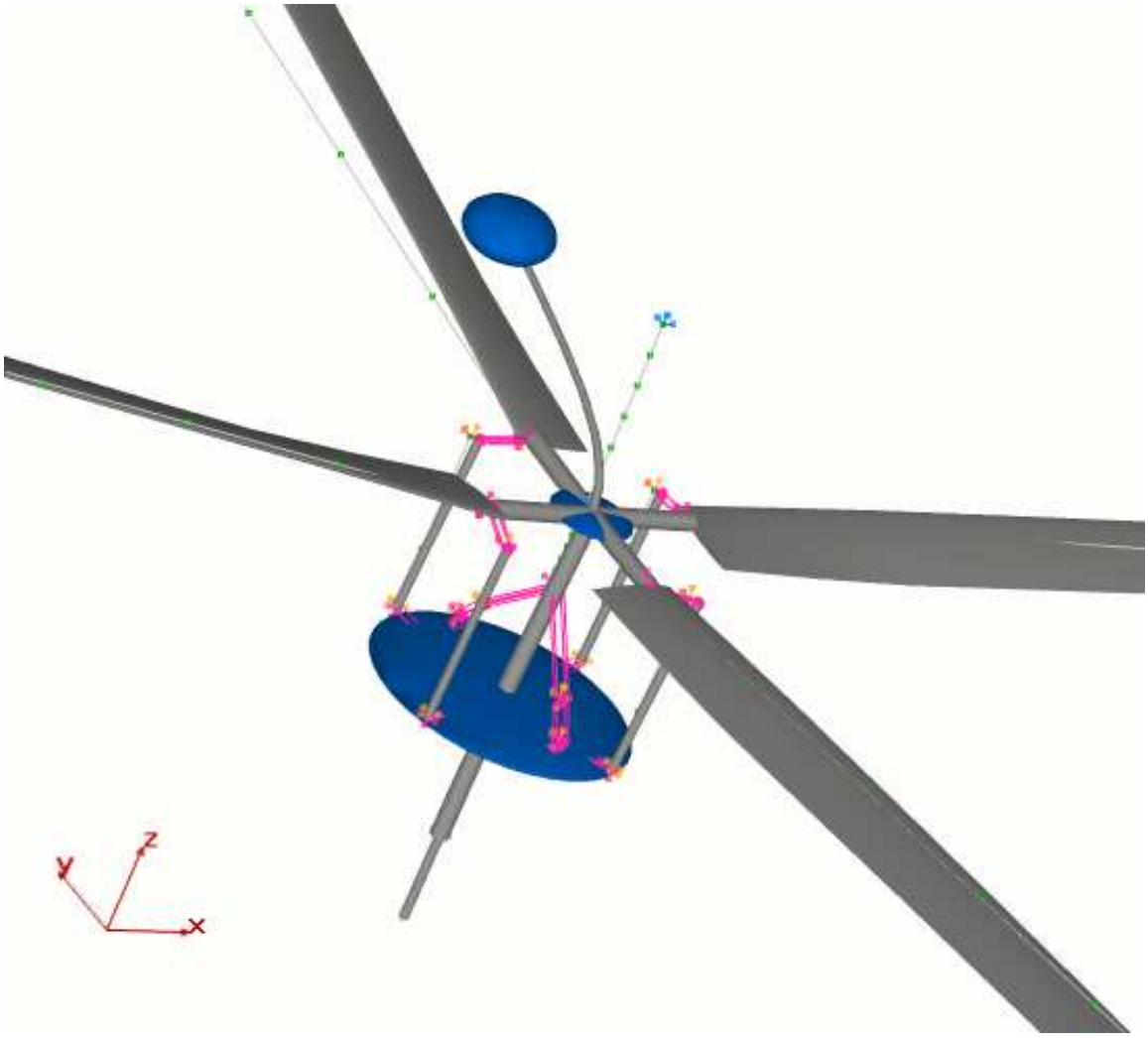

Figure 5: Eigenvector of the Floquet transition matrix corresponding to the unstable eigenvalue for $I_s = 1 \times 10^6$ lb·ft^2.

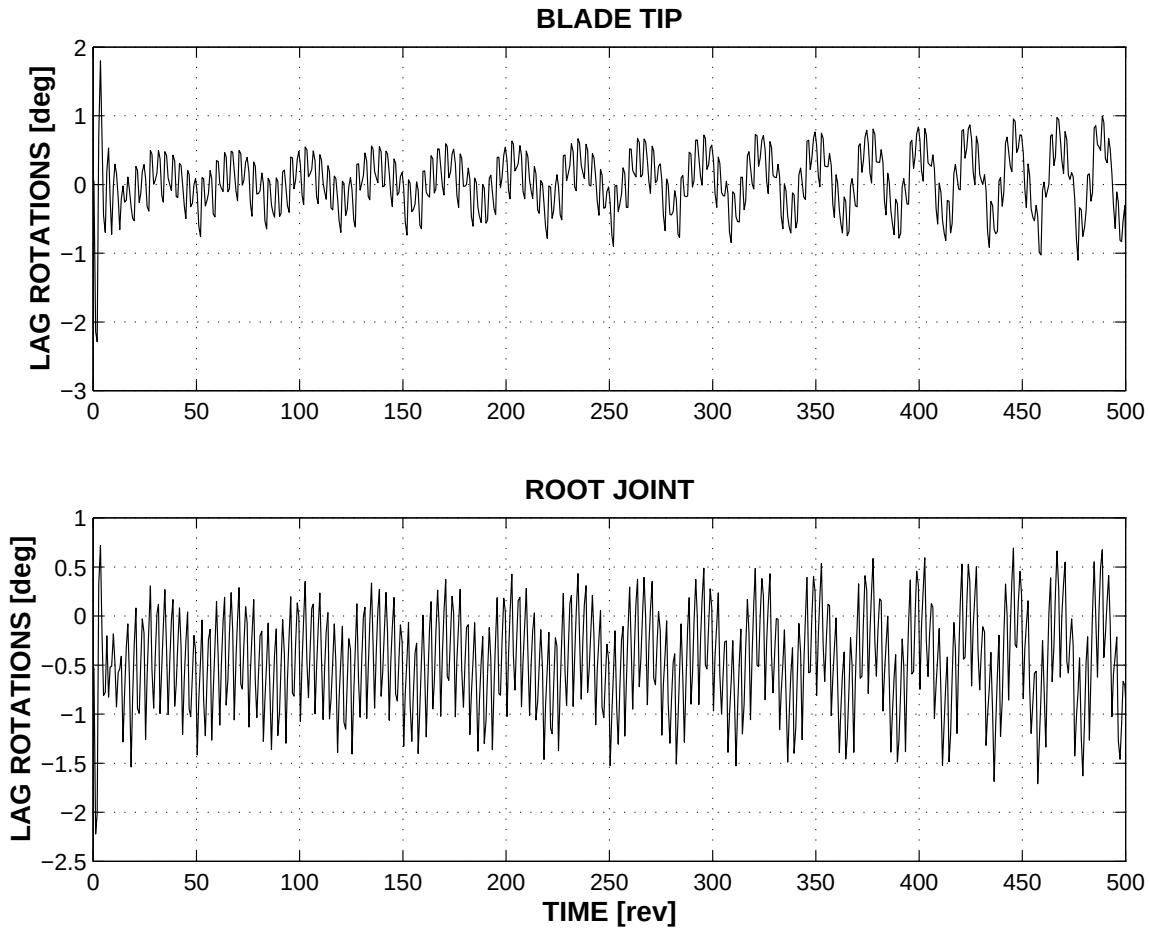

Figure 6: Time history of the blade tip lag rotation in a rotating coordinate system (top figure) and lag joint rotations (bottom figure). Shaft stifness $I_s = 1 \times 10^6\ lb.ft^2$.

the system does not clearly indicate a catastrophic increase in amplitude. Much longer integration periods would be required to detect the instability solely based on system response. This example clearly demonstrates that Floquet theory must be used for stability analysis of such systems. It also demonstrates the efficiency of the implicit Floquet theory: after 20 revolutions only, the five dominant eigenvalues of the system can be accurately determined. Furthermore, visualization of the eigenvectors of the transition matrix associated with the unstable eigenvalues provide valuable insight into the physical nature of the instability.

To study the influence of damping in joints on the stability, a simplified model of the rotor without shaft and control linkages was developed. The model included 456 degrees of freedom, corresponding to 756 states. Fig. 7 shows the frequencies and damping rates of the least-damped modes versus damping in joints. The study shows that the rotor does not exhibit instabilities even for small joint damping values.

6.2 Modeling a Variable Diameter Tilt-Rotor

This example deals with the modeling of a variable diameter tilt-rotor (VDTR) aircraft. Tilt-rotors are machines ideally suited to accomplish vertical take-off and landing missions characterized by high speed and long range. They operate either as a helicopter or as a propeller driven aircraft. The transition from one mode of operation to the other is achieved by tilting the engine nacelles. VDTR's further refine the tilt-rotor concept by introducing variable span blades to obtain optimum

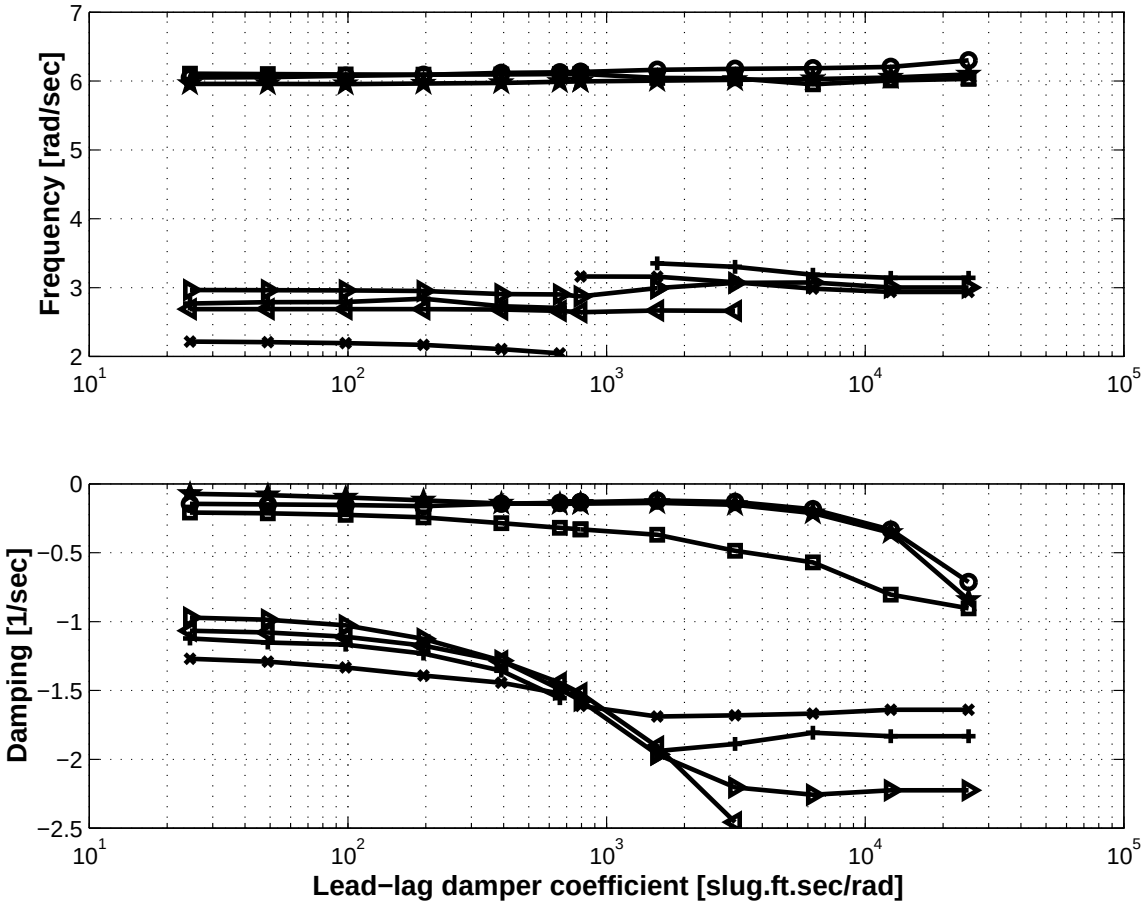

Figure 7: Frequencies and damping rates of the least-damped modes versus damping in joints.

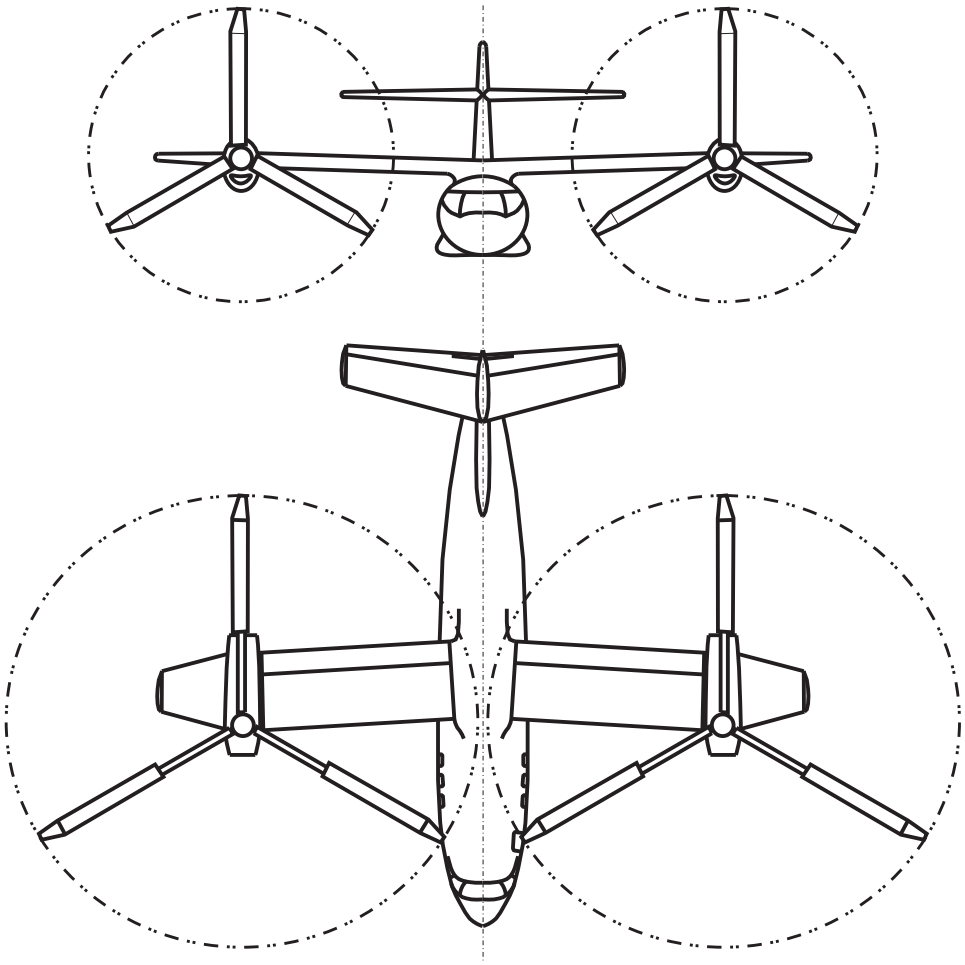

Figure 8: VDTR design schematic. Top figure: cruise configuration; bottom figure: hover configuration.

aerodynamic performance in both hover and cruise configurations. A general description of current VDTR technology is given in ref. [24], and fig. 8 schematically shows the proposed design.

Fig. 9 presents Sikorsky telescoping blade design. Fig. 10 depicts a schematic view of the multibody model of a typical VDTR configuration where a single blade only is shown, for clarity. A sliding joint and a sliding screw joint connect the swash-plate and the shaft. The motion of the swash-plate along the shaft controls the blade pitch through the pitch linkages. Prescribing the relative translation of the sliding joint, *i.e.* the translation of the swash-plate with respect to the shaft, controls the pitch setting, effectively transferring the pilot's command in the stationary system to the blade in the rotating system. The presence of a screw joint forces the swash-plate to rotate with the shaft while sliding along it. This is usually accomplished in a real system with a scissors-like mechanism that connects swash-plate and shaft. This level of detail in the model, although possible using beams and/or rigid bodies and revolute joints, was not considered to be necessary for the present analysis. A sliding screw joint models the nut-jackscrew assembly. The motion of the nuts along the jackscrew allows to vary the blade span in a continuous manner. By prescribing the relative translation at the joint, the blade can then be deployed or retracted according to a suitable function of the nacelle tilt. Finally, sliding screw joints are used to model the sliding contact between the torque tube and the outboard blade. Note that a sliding screw joint must be used here as the pilot's input is transferred from the linear motion of the swash-plate to twisting of the torque tubes through the pitch links, and finally to twisting of the outboard blade. Appropriate springs and dampers are provided at the gimbal, while springs are present at the flap

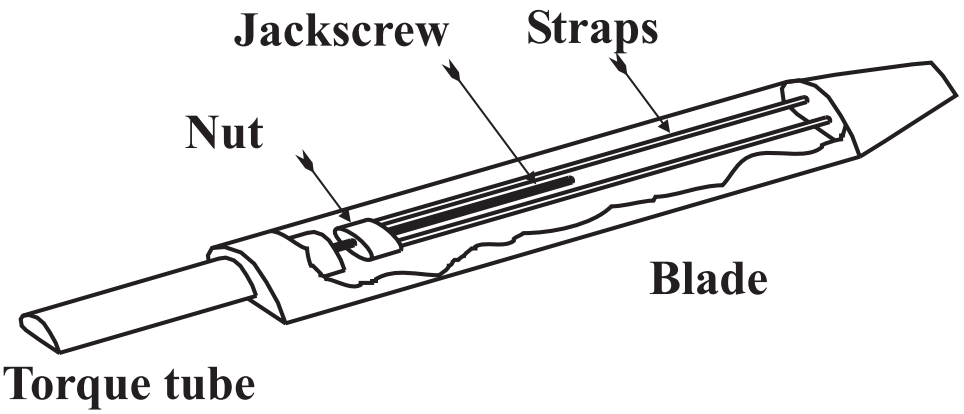

Figure 9: The Sikorsky telescoping blade design.

and lag revolute joints in order to correctly represent the characteristics of the system. Fig. 11 depicts the multibody representation of the problem.

Since actual data for this configuration is not yet available, the model used for this example has telescoping blades as in fig. 9, but the structural and aerodynamic characteristics are those of the XV-15 aircraft [43, 44]. Fig. 12 gives the variation of the thrust coefficient C_T in hover as function of the power coefficient C_P; good correlation with the experimental data is observed.

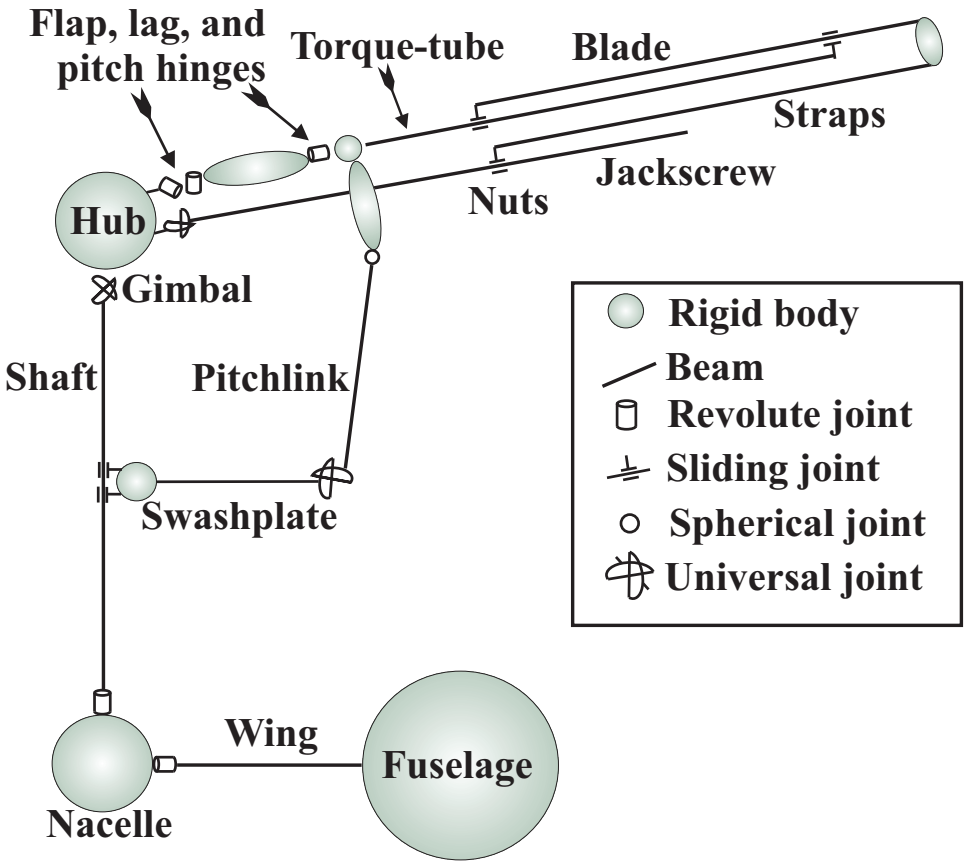

Figure 10: Configuration of the VDTR. For clarity, a single blade only is shown.

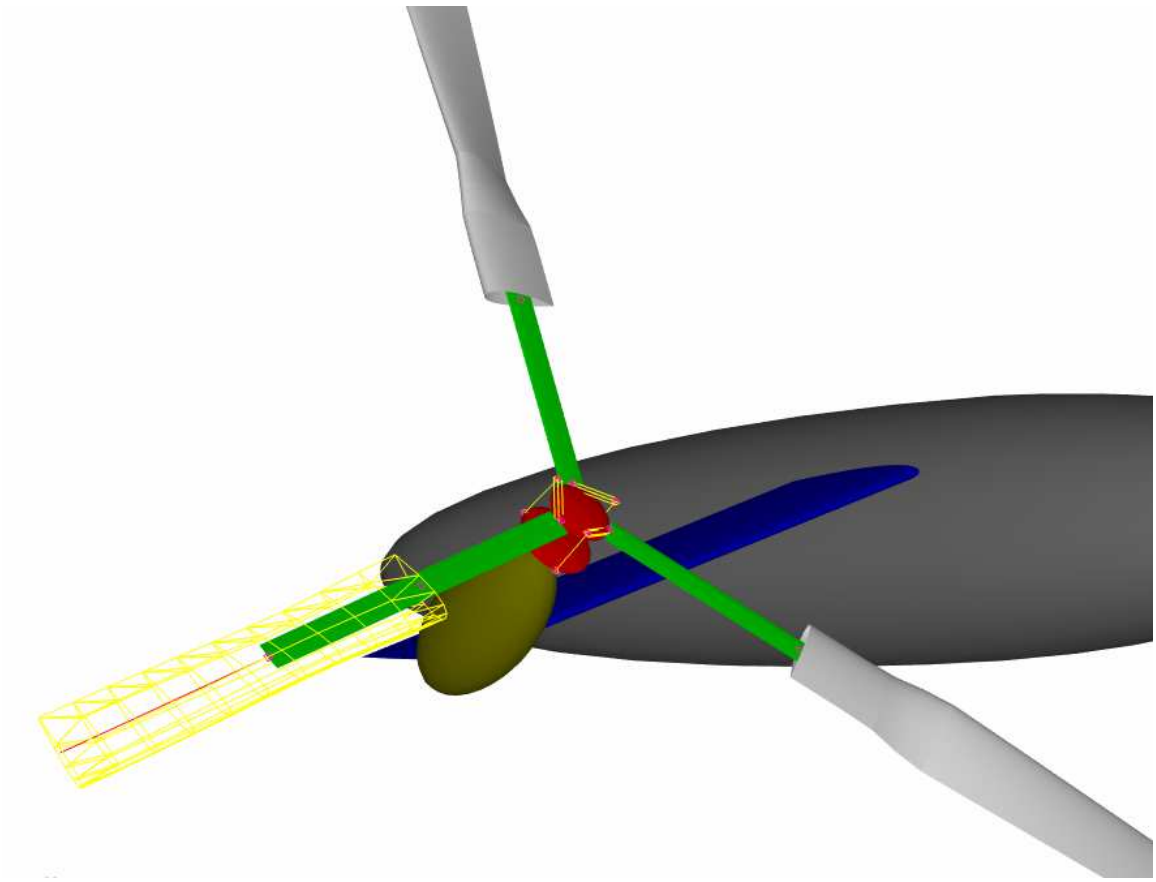

Figure 11: Graphical representation of the multibody model of the VDTR system.

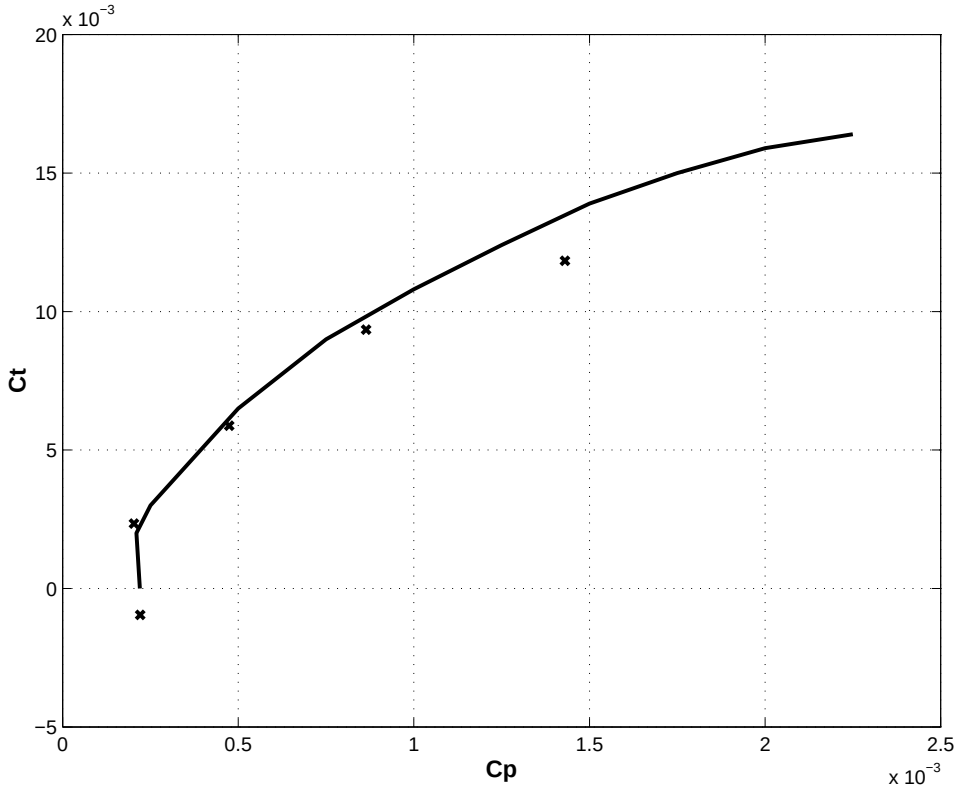

Figure 12: Thrust coefficient C_T versus power coefficient C_P and versus collective angle, for the VDTR model with XV-15 data.

The VDTR rotor is initially in the hover configuration, with the nacelles tilted upwards and the blades fully deployed. The rotor angular velocity is 20 rad/sec. The shaft rotational speed and blade pitch setting are kept constant while the nacelle is tilted forward to reach the cruise configuration. At the same time, the blades are retracted to avoid impact between the blade tips and the fuselage, and to optimize aerodynamic performance. The maneuver is completed in 20 sec, corresponding to about 64 revolutions of the rotor. The time history of the relative prescribed rotation at the wing-nacelle revolute joint is given as $\varphi = 0.25\,\pi\,(1 - \sin(2\,\pi(t/40 + 0.25))$, while the prescribed displacement at the nut-jackscrew sliding joint is linear in time. The retracted rotor diameter for cruise mode is 66% of that in hover. This simulation was conducted in a vacuum, *i.e.* without aerodynamics forces acting on the blades.

Fig. 13 gives a three dimensional view of the VDTR multibody model at four different time instants throughout the maneuver. This view is deceptively simple. In fact, the tilting of the nacelle involves a complex tilting motion of the gimbal with respect to the shaft. In turns, flapping, lagging and pitching motions of the blades are excited. The time history of one of the relative rotations at the gimbal is presented in fig. 14. The rotation about the other axis of the universal joint presents a similar behavior. As the nacelle begins its motion, gimbal rotations are excited and sharply increase during the first half of the conversion process. Then, the dampers present in the universal joint progressively decrease the amplitude of this motion. Fig. 15 shows the time history of the blade pitch. This pitching is entirely due to the gimbal tilting, since the swash-plate location along the shaft was fixed, which would imply a constant value of pitch for a rigid system. As expected, this motion closely follows the behavior of the gimbal. Fig. 16 shows the time history of lag hinge rotation which appears to be undamped. This is to be expected since there are no dampers in the lag hinges. Such motion would of course be damped by the aerodynamic forces.

Fig. 17 shows the time history of the force at the jackscrew-nut sliding joint during the blade retraction. Note that the jackscrew carries the entire centrifugal force. Indeed, the blade is free to slide with respect to the torque tube, and hence, no axial load is transmitted to this member. As a result, the variable span blade is subjected to compression during operation, a radical departure from classical designs in which blades operate in tension. As expected, fig. 17 shows that the axial load in the jackscrew decreases as the rotor diameter is reduced. The high frequency oscillating components of the signal are once again due to the flapping, lagging and tilting motions of blades and gimbal discussed above.

6.3 Rotorcraft tail rotor transmission

This last problem deals with the modeling of the supercritical tail rotor transmission of a helicopter. Fig. 18 shows the configuration of the problem. The aft part of the helicopter is modeled and consists of a 6 m fuselage section that connects at a 45 degree angle to a 1.2 m projected length tail section. This structure supports the transmission to which it is connected at points M and T by means of 0.25 m support brackets. The transmission is broken into two shafts, each connected to flexible couplings at either end. The flexible couplings are represented by flexible joints, consisting of concentrated springs and dampers. Shaft 1 is connected to a revolute joint at point S, and gear box 1 at point G. Shaft 2 is connected to gear box 1 and gear box 2 which in turns, transmits power to the tail rotor. The plane of the tail rotor is at a 0.3 m offset with respect to the plane defined by the fuselage and tail, and its hub is connected to gear box 2 by means of a short shaft. Each tail rotor blade has a length of 0.8 m and is connected to the rotor hub at point H through rigid root-attachments of length 0.2 m. The gear ratios for gear boxes 1 and 2 are 1:1 and 2:1, respectively.

The fuselage has the following physical characteristics: axial stiffness $EA = 687$ MN, bending stiffnesses $EI_{22} = 19.2\ \text{MN}\cdot\text{m}^2$, $EI_{33} = 26.9\ \text{MN}\cdot\text{m}^2$, torsional stiffness $GJ = 8.77\ \text{MN}\cdot\text{m}^2$, and mass per unit span $m = 15.65$ kg/m. The properties of the tail are one third of those of the fuselage.

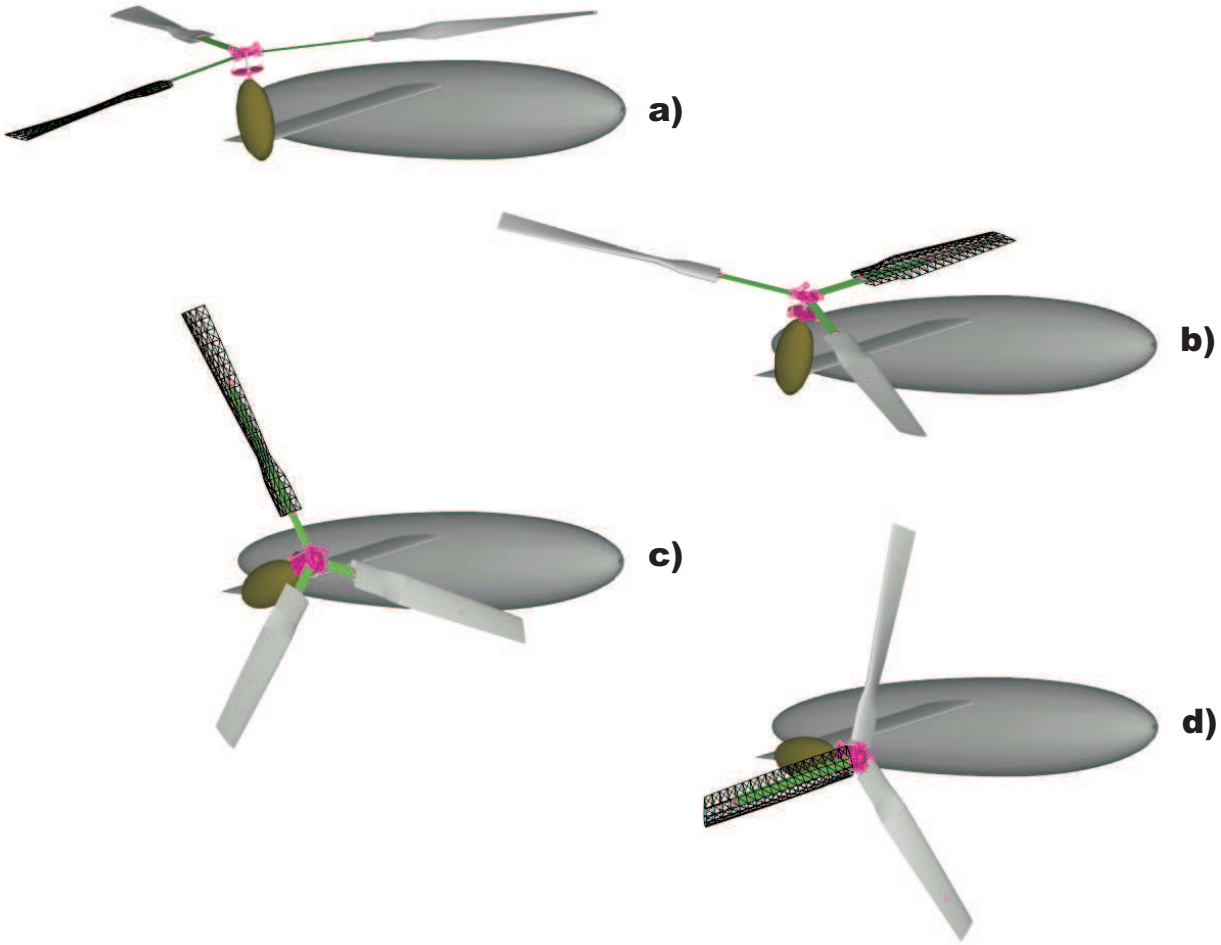

Figure 13: Snapshots of the VDTR multibody model during the conversion process from hover to airplane mode.

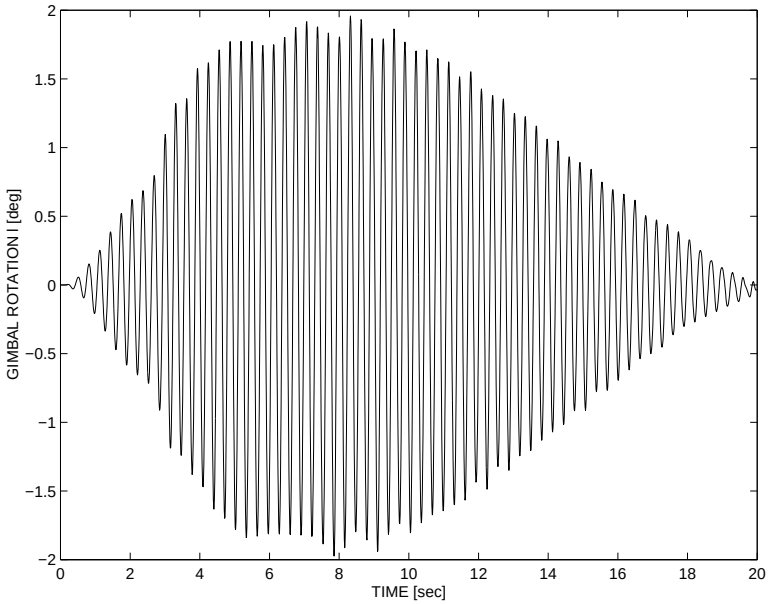

Figure 14: Time history of one of the relative rotations at the rotor gimbal.

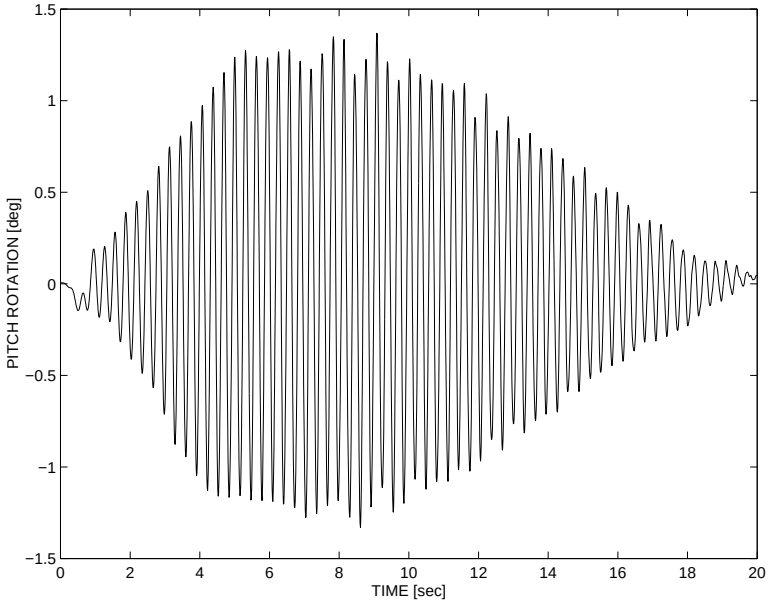

Figure 15: Time history of the relative rotations at the pitch hinge.

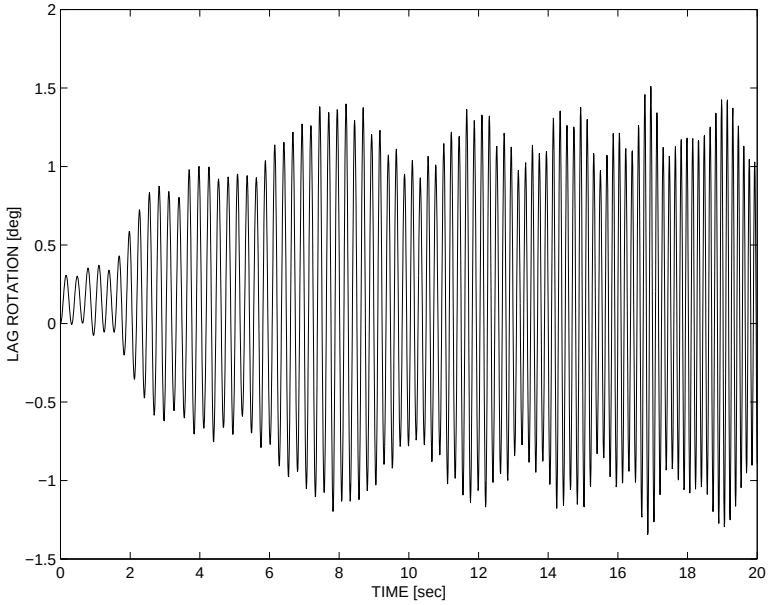

Figure 16: Time history of the relative rotations at the lag hinge.

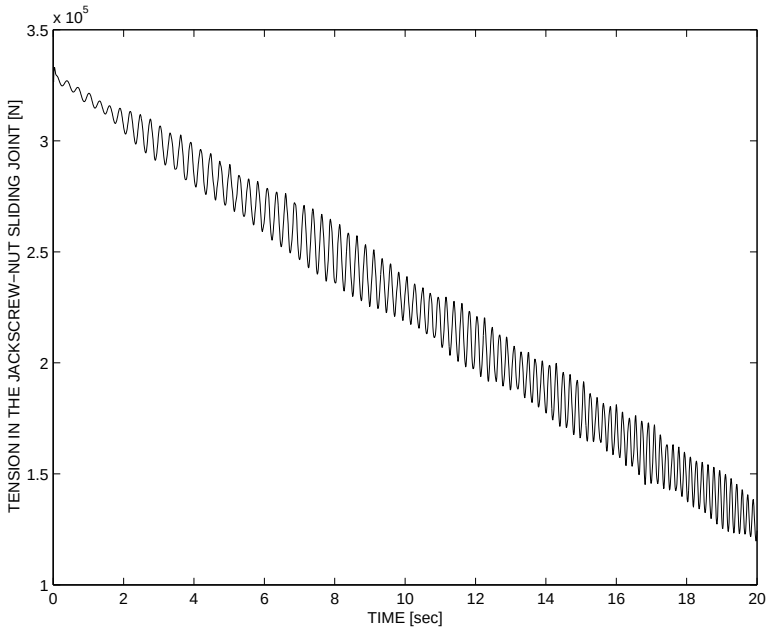

Figure 17: Time history of the force at jackscrew-nut sliding joint during blade retraction.

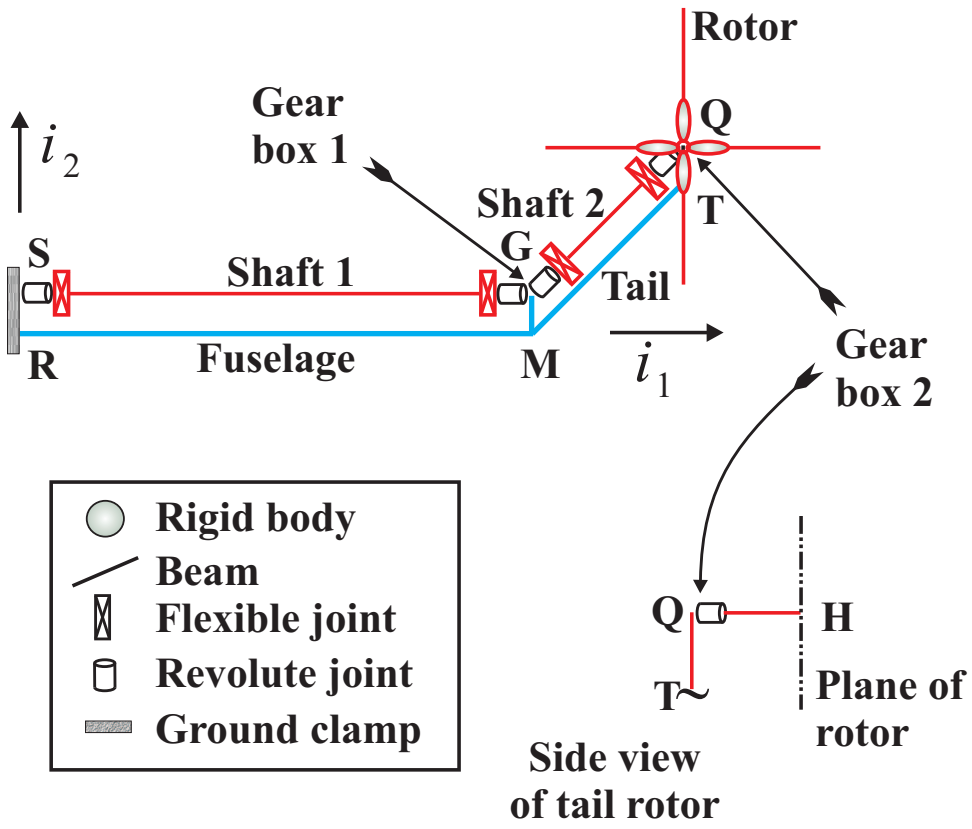

Figure 18: Configuration of a tail rotor transmission.

Shafts 1 and 2 have the following physical characteristics: axial stiffness $EA = 22.9$ MN, bending stiffnesses $EI_{22} = 26.7$ kN·m^2 and $EI_{33} = 27.7$ kN·m^2, torsional stiffness $GJ = 22.1$ kN·m^2, and mass per unit span $m = 0.848$ kg/m. The center of mass of the shaft has a 1 mm offset with respect to the shaft reference line. The small difference in bending stiffnesses together with the center of mass offset are meant to represent an initial manufacturing imperfection or an unbalance in the shaft. The stiffness and damping properties of the flexible couplings are as follows: axial stiffness 5.0 kN/m and damping 0.5 N·sec/m, transverse stiffnesses 1.0 MN/m and damping 100 N·sec/m, torsional stiffness 0.1 MN·m/rad and damping 10 N·m·sec/rad, and bending stiffnesses 0.1 kN·m/rad and damping 0.01 N·m·sec/rad. Finally, gear boxes 1 and 2 have a concentrated mass of 5.0 kg each, and the tail rotor a 15.0 kg mass with a polar moment of inertia of 3.0 kg·m^2.

At first, a static analysis of the system was performed for various constant angular velocities of the drive train. The natural frequencies of the system were computed about each equilibrium configuration. Fig. 19 shows the two lowest modes of both fuselage and shaft. The two lowest natural frequencies of shaft 1 were found to be $\omega_1 = 46.9$ and $\omega_2 = 49.1$ rad/sec. According to linear theory, the system is stable when the shaft angular velocity is below ω_1 or above ω_2, but unstable between theses two speeds.

Next, a dynamic simulation was performed; the initial condition of the simulation was selected as the static equilibrium configuration of the system for an angular velocity $\Omega = 45$ rad/sec of the drive train. A torque Q is applied to shaft 1 at point S and has the following time history

$$Q(t) = \begin{cases} 0 & t < 1 \ sec, \\ 12\ (1 - cos\ 2\pi t) & 1 < t < 2 \ sec, \\ 0 & t > 2 \ sec. \end{cases} \tag{3}$$

The simulation was run with a constant time step $\Delta t = 5 \times 10^{-04}$ *sec*, for a total time of 5 sec, corresponding to about 40 revolutions of shaft 1. Shaft 1 initially operates in a stable regime, $\Omega = 45$ rad/sec, then accelerates due to the applied torque, and rapidly reaches a speed of $\Omega = 50.5$ rad/sec, past the critical speed range. Fig. 20 shows the time history of shaft 1 and 2 angular velocities; the horizontal lines indicate the unstable zone. The motion of shaft 1 mid-span point, projected onto the $\bar{\imath}_2$, $\bar{\imath}_3$ plane, is depicted in fig. 21 which shows the whirling motion associated with the crossing of the critical speed zone. Of course, shaft 1 motions induce vibrations in the fuselage as shown in fig. 22 that depicts the time history of tail tip transverse displacements. Note the dramatic rise in amplitude when the shaft reaches the critical speed. Since the only dissipation in the system comes from the small amount of viscous damping present in the flexible joints, shaft vibrations continue above the critical speed.

The large amplitude vibrations of shaft 1 during the crossing of the critical speed zone generate significant mid-span bending moments that are depicted in fig. 23. Of course, these vibrations induce large loads at the fuselage root section; fig. 24 shows the fast Fourier transform of the fuselage root bending moment. Note the large peak at the shaft natural frequency of about 49 *rad/sec*, together with smaller peaks at integer multiples thereof, due to the nonlinearities of the system.

7 Conclusions

This paper has described a multibody dynamics approach to the modeling of rotorcraft systems. This approach allows the modeling of complex configurations of arbitrary topology through the assembly of basic components chosen from an extensive library of elements that includes rigid and deformable bodies as well as joint elements.

Deformable bodies, such as beams and shells, are modeled with the finite element method, without resorting to modal approximations, in contrast with both rotorcraft and multibody common

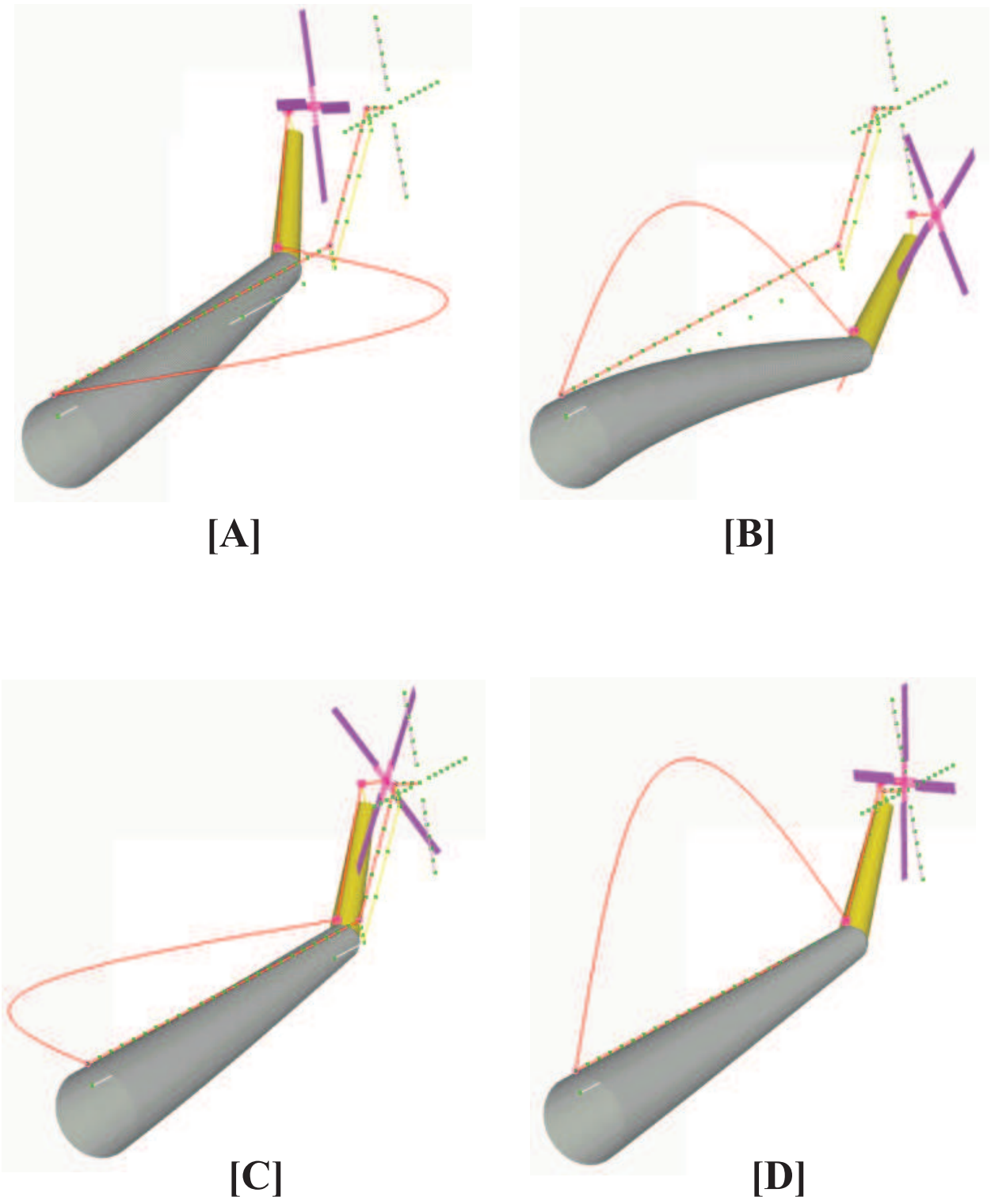

Figure 19: Eigen modes of the rotorcraft tail rotor transmission system. [**A**] and [**B**]: two lowest fuselage bending modes at 51.90 and 61.03 rad/sec, respectively. [**C**] and [**D**]: two lowest shaft bending modes at 46.91 and 49.09 rad/sec.

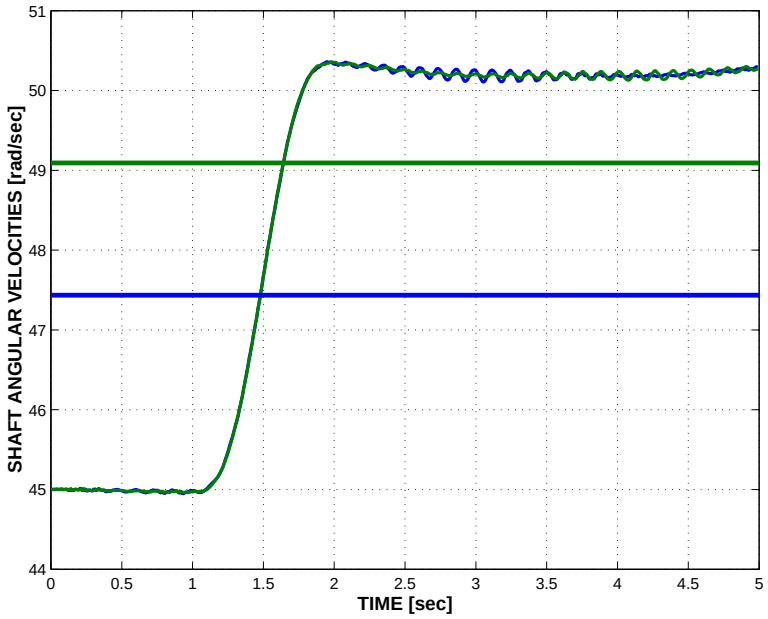

Figure 20: Time history of shaft 1 (solid line) and 2 (dashed line) angular velocities.

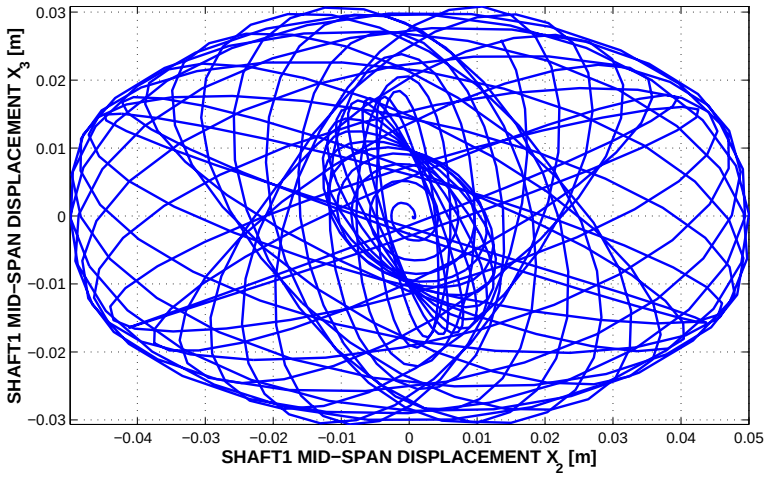

Figure 21: Whirling motion of shaft 1 mid-span point.

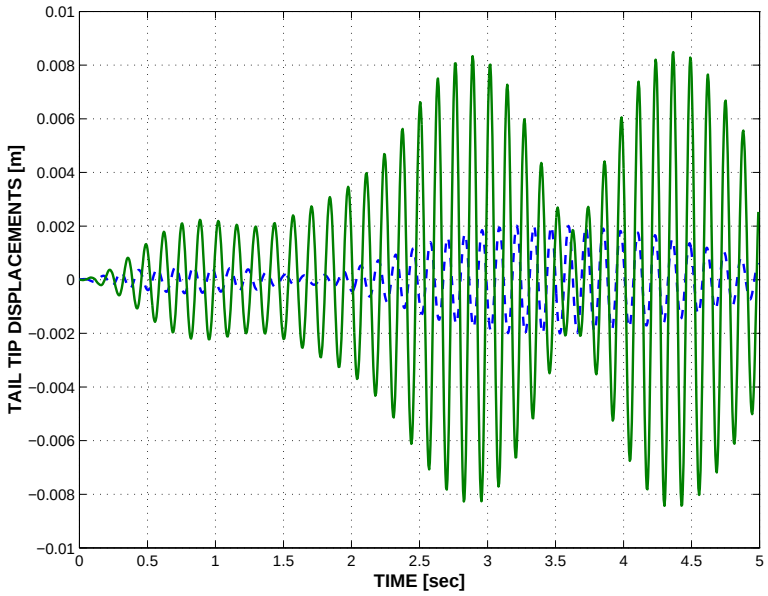

Figure 22: Motion of the tip point of the tail section. Vertical motion: solid line; horizontal motion: dashed line.

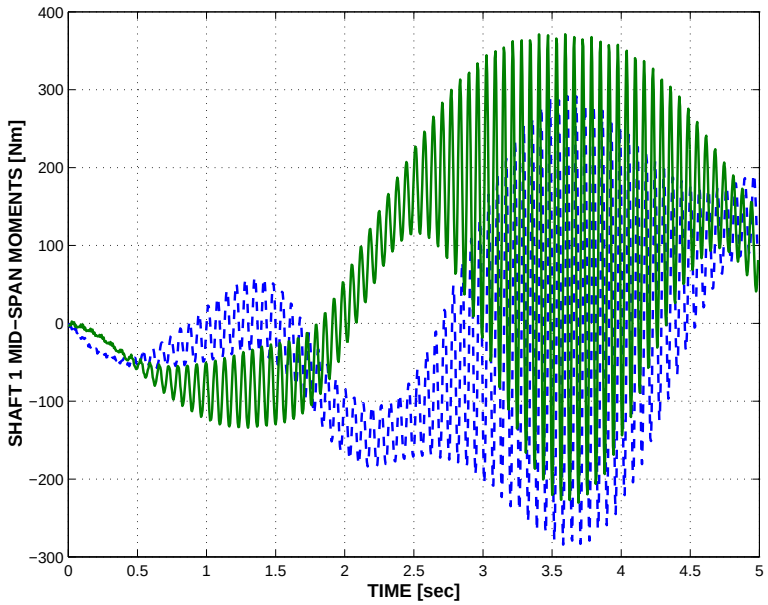

Figure 23: Shaft mid-span bending moments measured a body attached coordinate system; M_2: solid line, M_3 dashed line.

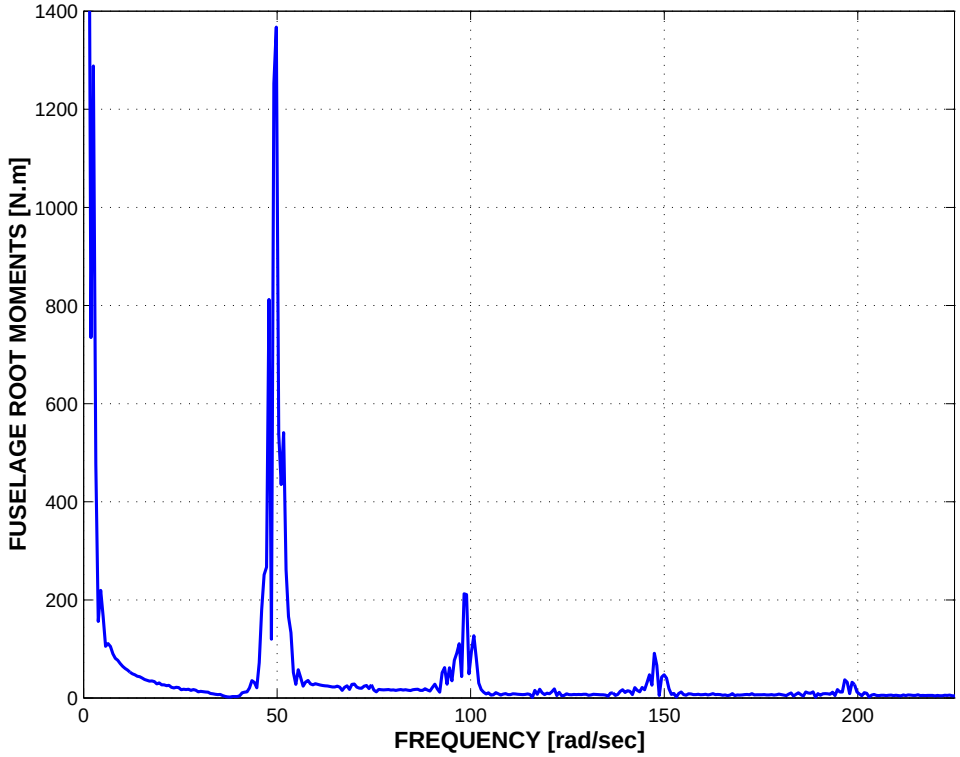

Figure 24: Fast Fourier transform of the fuselage root bending moment.

modeling practices. Efficient algorithms and advances in computer hardware enable the analysis of complex configurations on desktop personal computers.

A distinguishing feature of multibody systems is the presence of a number of joints that impose constraints on the relative motion of the various bodies of the system. The lower pair joints, *i.e.* the revolute, prismatic, screw, cylindrical, planar and spherical joints are sufficient to model most classical rotorcraft configurations. More advanced joints, such as sliding joints or contact and backlash elements might be needed to deal with unusual problems and configurations.

A key element of the formulation is the development of robust and efficient time integration algorithms for dealing with the large scale, nonlinear, differential/algebraic equations resulting from the proposed formulation. Static, dynamic, stability, and trim analyses can be performed on the models. Furthermore, efficient post-processing and visualization tools are available to obtain physical insight into the dynamic response of the system that can be obscured by the massive amounts of data generated by multibody simulations.

Multibody formulations are now well established and can deal with complex rotorcraft configurations of arbitrary topology. This new approach to rotorcraft dynamic analysis seems to be very promising since it enjoys all the characteristics that made the finite element method the most widely used and trusted simulation tool in many different engineering disciplines and areas. This new paradigm for rotorcraft analysis is expected to gain popularity and become an industry standard in the years to come.

References

[1] P.E. Nikravesh. *Computer-Aided Analysis of Mechanical Systems*. Prentice-Hall, Englewood Cliffs, New Jersey, 1988.

[2] F.M.L. Amirouche. *Computational Methods in Multibody Dynamics*. Prentice-Hall, Englewood Cliffs, New Jersey, 1992.

[3] J.C. Houbolt and G.W. Brooks. Differential equations of motion for combined flapwise bending, chordwise bending, and torsion of twisted nonuniform rotor blades. Technical Report 1348, NACA Report, 1958.

[4] D.H. Hodges and E.H. Dowell. Nonlinear equations of motion for the elastic bending and torsion of twisted nonuniform rotor blades. Technical report, NASA TN D-7818, 1974.

[5] O.A. Bauchau and D.H. Hodges. Analysis of nonlinear multi-body systems with elastic couplings. *Multibody System Dynamics*, 3(2):168–188, May 1999.

[6] W.O. Schiehlen. Multibody system dynamics: Roots and perspectives. *Multibody System Dynamics*, 1:149–188, 1997.

[7] A.A. Shabana. Flexible multibody dynamics: Review of past and recent developments. *Multibody System Dynamics*, 1(2):189–222, June 1997.

[8] O.A. Bauchau and D. Guernsey. On the choice of appropriate bases for nonlinear dynamic modal analysis. *Journal of the American Helicopter Society*, 38(4):28–36, 1993.

[9] O.A. Bauchau and W.Y. Chiang. Dynamic analysis of rotor flexbeams based on nonlinear anisotropic shell models. *Journal of the American Helicopter Society*, 38(1):55–61, January 1993.

[10] O.A. Bauchau and W.Y. Chiang. Dynamic analysis of bearingless tail-rotor blades based on nonlinear shell models. *Journal of Aircraft*, 31(6):1402–1410, November-December 1994.

[11] V.L. Berdichevsky. On the energy of an elastic rod. *Prikladnaya Matematika y Mekanika*, 45(4):518–529, 1982.

[12] C.E.S. Cesnik and D.H. Hodges. VABS: A new concept for composite rotor blade cross-sectional modeling. *Journal of the American Helicopter Society*, 42(1):27–38, January 1997.

[13] V. Giavotto, M. Borri, P. Mantegazza, G. Ghiringhelli, V. Carmaschi, G.C. Maffioli, and F. Mussi. Anisotropic beam theory and applications. *Computers & Structures*, 16(1-4):403–413, 1983.

[14] M. Borri and T. Merlini. A large displacement formulation for anisotropic beam analysis. *Meccanica*, 21:30–37, 1986.

[15] D.H. Hodges. A review of composite rotor blade modeling. *AIAA Journal*, 28(3):561–565, March 1990.

[16] O.A. Bauchau and N.J. Theron. Energy decaying scheme for non-linear beam models. *Computer Methods in Applied Mechanics and Engineering*, 134(1-2):37–56, 1996.

[17] C.L. Bottasso and M. Borri. Integrating finite rotations. *Computer Methods in Applied Mechanics and Engineering*, 164:307–331, 1998.

[18] O.A. Bauchau and C.L. Bottasso. On the design of energy preserving and decaying schemes for flexible, nonlinear multi-body systems. *Computer Methods in Applied Mechanics and Engineering*, 169(1-2):61–79, 1999.

[19] V.G. Sutyrin. Derivation of plate theory accounting asymptotically correct shear deformation. *Journal of Applied Mechanics*, 64:905–915, 1997.

[20] O.A. Bauchau, C.L. Bottasso, and L. Trainelli. Robust integration schemes for flexible multi-body systems. *Computer Methods in Applied Mechanics and Engineering*, 192(3-4):395–420, 2003.

[21] J. Angeles. *Spatial Kinematic Chains*. Springer-Verlag, Berlin, 1982.

[22] O.A. Bauchau. On the modeling of prismatic joints in flexible multi-body systems. *Computer Methods in Applied Mechanics and Engineering*, 181(1-3):87–105, 2000.

[23] O.A. Bauchau and C.L. Bottasso. Contact conditions for cylindrical, prismatic, and screw joints in flexible multi-body systems. *Multibody System Dynamics*, 5:251–278, 2001.

[24] E.A. Fradenburgh and D.G. Matuska. Advancing tiltrotor state-of-the-art with variable diameter rotors. In *American Helicopter Society 48th Annual Forum Proceedings*, Washington, D.C., June 3-5 1992.

[25] O.A. Bauchau. Analysis of flexible multi-body systems with intermittent contacts. *Multibody System Dynamics*, 4:23–54, 2000.

[26] O.A. Bauchau. On the modeling of friction and rolling in flexible multi-body systems. *Multibody System Dynamics*, 3:209–239, 1999.

[27] O.A. Bauchau and J. Rodriguez. Simulation of wheels in nonlinear, flexible multi-body systems. *Multibody System Dynamics*, 7:407–438, 2002.

[28] O.A. Bauchau and J.U. Ahmad. Advanced CFD and CSD methods for multidisciplinary applications in rotorcraft problems. In *Proceedings of the AIAA/NASA/USAF Multidisciplinary Analysis and Optimization Symposium*, pages 945–953, 1996.

[29] H. Murty, C.L. Bottasso, M. Dindar, M.S. Shephard, and O.A. Bauchau. Aeroelastic analysis of rotor blades using nonlinear fluid/structure coupling. In *American Helicopter Society 53rd Annual Forum Proceedings*, Virginia Beach, VA, April 1997.

[30] E. Hairer and G. Wanner. *Solving Ordinary Differential Equations II : Stiff and Differential-Algebraic Problems*. Springer, Berlin, 1996.

[31] O.A. Bauchau and N.J. Theron. Energy decaying schemes for nonlinear elastic multi-body systems. *Computers & Structures*, 59(2):317–331, 1996.

[32] C.L. Bottasso and M. Borri. Energy preserving/decaying schemes for non-linear beam dynamics using the helicoidal approximation. *Computer Methods in Applied Mechanics and Engineering*, 143:393–415, 1997.

[33] O.A. Bauchau and T. Joo. Computational schemes for nonlinear elasto-dynamics. *International Journal for Numerical Methods in Engineering*, 45(6):693–719, 1999.

[34] O.A. Bauchau. Computational schemes for flexible, nonlinear multi-body systems. *Multibody System Dynamics*, 2(2):169–225, 1998.

[35] M. Borri, C.L. Bottasso, and L. Trainelli. A novel momentum-preserving energy-decaying algorithm for finite element multibody procedures. In Jorge Ambrósio and Michal Kleiber, editors, *Proceedings of Computational Aspects of Nonlinear Structural Systems with Large Rigid Body Motion, NATO Advanced Research Workshop, Pultusk, Poland, July 2-7*, pages 549–568, 2000.

[36] G.H. Gaonkar and D.A. Peters. Review of Floquet theory in stability and response analysis of dynamic systems with periodic coefficients. In *R.L. Bisplinghoff Memorial Symposium Volume on Recent Trends in Aeroelasticity, Structures and Structural Dynamics, Feb 6-7, 1986*, pages 101–119. University Press of Florida, Gainesville, 1986.

[37] O.A. Bauchau and Y.G. Nikishkov. An implicit Floquet analysis for rotorcraft stability evaluation. *Journal of the American Helicopter Society*, 46:200–209, 2001.

[38] O.A. Bauchau and Y.G. Nikishkov. An implicit transition matrix approach to stability analysis of flexible multibody systems. *Multibody System Dynamics*, 5:279–301, 2001.

[39] D.A. Peters. Flap-lag stability of helicopter rotor blades in forward flight. *Journal of the American Helicopter Society*, 20(4), 1975.

[40] D.A. Peters and D. Barwey. A general theory of rotorcraft trim. *Mathematical Problems in Engineering*, 2:1–34, 1996.

[41] D.A. Peters and C.J. He. Finite state induced flow models. Part II: Three-dimensional rotor disk. *Journal of Aircraft*, 32(2):323–333, 1995.

[42] R.G. Loewy and M. Zotto. Helicopter ground/air resonance including rotor shaft flexibility and control coupling. In *American Helicopter Society 45th Annual Forum Proceedings*, Boston, MA, May 1989.

[43] C.W. Acree and M.B. Tischler. Determining xv-15 aeroelastic modes from flight data with frequency-domain methods. Technical Report TP 3330, ATCOM TR 93-A-004, NASA, 1993.

[44] K. Bartie, H. Alexander, M. McVeigh, S. La Mon, and H. Bishop. Hover performance tests of baseline metal and advanced technology blade (ATB) rotor systems for the xv-15 tilt rotor aircraft. Technical Report CR 177436, NASA, 1982.